land

MDPI

Article

Ozone Response of Leaf Physiological and Stomatal Characteristics in *Brassica juncea* L. at Supraoptimal Temperatures

Jong Kyu Lee [1], Myeong Ja Kwak [1], Sang Hee Park [1], Han Dong Kim [1], Yea Ji Lim [1], Su Gyeong Jeong [1], Yun Soo Choi [2] and Su Young Woo [1,*]

[1] Department of Environmental Horticulture, University of Seoul, Seoul 02504, Korea; gpl90@naver.com (J.K.L.); 016na8349@hanmail.net (M.J.K.); gosowk0930@uos.ac.kr (S.H.P.); khd1992@uos.ac.kr (H.D.K.); g201942002@uos.ac.kr (Y.J.L.); tnrud2401@uos.ac.kr (S.G.J.)
[2] Department of Geoinformatics, University of Seoul, Seoul 02504, Korea; choiys@uos.ac.kr
* Correspondence: wsy@uos.ac.kr; Tel.: +82-10-3802-5242

Abstract: Plants are affected by the features of their surrounding environment, such as climate change and air pollution caused by anthropogenic activities. In particular, agricultural production is highly sensitive to environmental characteristics. Since no environmental factor is independent, the interactive effects of these factors on plants are essential for agricultural production. In this context, the interactive effects of ozone (O_3) and supraoptimal temperatures remain unclear. Here, we investigated the physiological and stomatal characteristics of leaf mustard (*Brassica juncea* L.) in the presence of charcoal-filtered (target concentration, 10 ppb) and elevated (target concentration, 120 ppb) O_3 concentrations and/or optimal (22/20 °C day/night) and supraoptimal temperatures (27/25 °C). Regarding physiological characteristics, the maximum rate of electron transport and triose phosphate use significantly decreased in the presence of elevated O_3 at a supraoptimal temperature (OT conditions) compared with those in the presence of elevated O_3 at an optimal temperature (O conditions). Total chlorophyll content was also significantly affected by supraoptimal temperature and elevated O_3. The chlorophyll *a*/*b* ratio significantly reduced under OT conditions compared to C condition at 7 days after the beginning of exposure (DAE). Regarding stomatal characteristics, there was no significant difference in stomatal pore area between O and OT conditions, but stomatal density under OT conditions was significantly increased compared with that under O conditions. At 14 DAE, the levels of superoxide (O_2^-), which is a reactive oxygen species, were significantly increased under OT conditions compared with those under O conditions. Furthermore, leaf weight was significantly reduced under OT conditions compared with that under O conditions. Collectively, these results indicate that temperature is a key driver of the O_3 response of *B. juncea* via changes in leaf physiological and stomatal characteristics.

Keywords: *Brassica juncea* L.; ozone; physiological characteristics; stomatal characteristics; supraoptimal temperature

check for updates

Citation: Lee, J.K.; Kwak, M.J.; Park, S.H.; Kim, H.D.; Lim, Y.J.; Jeong, S.G.; Choi, Y.S.; Woo, S.Y. Ozone Response of Leaf Physiological and Stomatal Characteristics in *Brassica juncea* L. at Supraoptimal Temperatures. *Land* **2021**, *10*, 357. https://doi.org/10.3390/land10040357

Academic Editor: Sofia Bajocco

Received: 22 February 2021
Accepted: 20 March 2021
Published: 1 April 2021

Publisher's Note: MDPI stays neutral with regard to jurisdictional claims in published maps and institutional affiliations.

Copyright: © 2021 by the authors. Licensee MDPI, Basel, Switzerland. This article is an open access article distributed under the terms and conditions of the Creative Commons Attribution (CC BY) license (https://creativecommons.org/licenses/by/4.0/).

1. Introduction

Over the next 40 years, the demand for agricultural production is expected to increase by at least 50% as a result of the projected growth of human population [1]. However, agricultural production is highly sensitive to environmental characteristics [2]. According to the latest Intergovernmental Panel on Climate Change (IPCC) Fifth Assessment Report, anthropogenic activities, such as rapid industrial development, have led to substantial climate change due to increased greenhouse gas emission [3]. The global mean temperature is expected to increase by 1.1 °C to 4.8 °C depending on future climate scenarios within this century, which will further worsen global warming and its associated problems related

to the ecosystems and crops [3,4]. Climate change is a critical threat to ecosystem health. In particular, global warming may severely damage agricultural crops [4].

To combat global warming, the responses of agricultural crops to increased temperatures in the future must be investigated. Prolonged exposure to elevated temperatures is a critical threat to global crop production [5]. Depending on their developmental stages and specific characteristics, plants respond differently to temperature. However, temperatures exceeding the upper tolerance threshold of plants decrease their net photosynthetic rate and total biomass [6]. Given the importance of temperature in determining net carbon metabolism [7], supraoptimal temperatures can negatively affect plant growth and development. In general, high temperatures increase respiration and photorespiration and possibly deactivate ribulose 1,5-bisphosphate carboxylase/oxygenase (RuBisCO) to limit photosynthesis. There are two reasons for the increased photorespiration and suppressed photosynthesis under elevated temperatures. First, high temperature decreases the specificity of RuBisCO for CO_2 relative to that for O_2, promoting rapid oxygenation. Next, the solubility of O_2 decreases more slowly than that of CO_2 [8]. In addition, the imbalance between photosynthesis and respiration impairs plant growth under elevated temperatures [9].

Furthermore, elevated environmental temperatures can increase stomatal movement, which is linked to primary metabolism [10]. Plant stomatal processes play pivotal roles in carbon cycles [11]. In particular, stomatal conductance is one of the important factors influencing plant net photosynthetic rate and carbon metabolism. However, previous experiments assessing the direct dependence of stomatal conductance on temperature have achieved inconsistent results [12]. In general, stomatal characteristics are strongly affected by elevated temperatures [13]. Recent studies have reported that plants can acclimate to warmer conditions by regulating the interaction between stomatal movement and vapor pressure deficit to allow growth and photosynthesis [14,15]. As a result of these physiological changes, plant growth and development are suppressed at supraoptimal temperatures, which further reduces the total biomass and yield of crops [16].

In addition, tropospheric ozone (O_3) concentration is expected to rise along with global warming, since the levels of O_3 precursors, such as NO_x, CO, and volatile organic compounds, are predicted to increase in the future [17]. Currently, O_3 is more harmful to agricultural crops than other air pollutants. Specifically, elevated O_3 levels may impede plant physiological processes, including photosynthesis [18]. Plants grown in the presence of elevated O_3 levels show decreased carbon metabolism [19]. In particular, photosynthetic inhibition by O_3 exposure has been attributed to reduced carboxylation efficiency, impaired electron transport, and dysregulated stomatal movement. Consequently, the levels of nonstructural carbohydrates, including sucrose and starch, are reduced [20]. In addition to decreased carbon availability, O_3-induced stress indirectly affects the carbon balance in plant cells via reactive oxygen species (ROS) generation [21].

The rate of O_3 influx to leaves is controlled by the stomatal aperture. Typically, stomatal closure is recognized as a response to limit O_3 uptake. Acute O_3 exposure can substantially decrease stomatal conductance via ROS accumulation in the guard cells [22]. Several studies using open-top chamber experiments have reported that O_3 decreases stomatal conductance, consequently limiting CO_2 influx to leaves [23,24]. Nonetheless, this mechanism is not supported by the results of other experiments. Some studies have reported that stomata cannot rapidly close as a result of impairment following exposure to high O_3 concentrations [25,26]. Elevated O_3 may delay the stomatal response by delignifying the guard cells and reducing abscisic acid (ABA) sensitivity [26]. The ABA response of stomata is associated with O_3-induced ethylene emission [27]. Regardless of the mechanisms involved, O_3 is evidently an important determinant of plant physiology.

Individual effects of supraoptimal temperatures and O_3 levels are unlikely to occur in natural environments, because neither factor acts independently on plants [28]. As such, tropospheric O_3 concentration shows a linear relationship with atmospheric temperature [29]. In addition, elevated O_3 is related to increased temperature, which can

directly affect the chemical kinetics and mechanisms of O_3 formation [30]. Environmental factors can synergistically affect plant responses, which cannot be predicted based on the results of experiments on individual factors [31]. Although recent studies have proven the individual effects of O_3 or temperature on plants, their interactive effects remain relatively understudied [5,7,19,32]. Furthermore, in addition to greenhouses, agricultural crops are cultivated on open fields, where they are highly prone to exposure to elevated temperatures and O_3 concentrations. Therefore, the interactive effects of these two environmental factors on crops warrant close attention.

To this end, the present study examined the individual and combined effects of supraoptimal temperatures and elevated O_3 concentrations in leaf mustard (*Brassica juncea* L.), which is widely cultivated in East Asia. Leaf mustard *B. juncea* is a biennial vegetable crop usually used for edible leaves and seeds to make mustard [33]. The effects of elevated O_3 have been largely researched on *Brassica* species throughout the world [34–37]. Singh et al. [37] reported observed decreases in photosynthetic rate and nutrient levels of *Brassica campesteris* L. var. Kranti under ambient O_3 ranging from 40 to 52 ppb at field condition. Singh et al. [38] also studied the synergistic effects of elevated O_3 and CO_2 on yield and photosynthetic rate of *Brassica juncea*. There is not sufficient research to assess the effects of O_3 and temperature on the physiological changes of *B. juncea*. Specifically, we investigated the effects of optimal and supraoptimal temperatures and/or ambient and elevated O_3 concentrations on the physiological and stomatal characteristics of leaf mustard and observed whether supraoptimal temperatures alter the O_3 responses of plants by regulating stomatal movement and carbon metabolism. We hypothesized that (i) the interactive effects of supraoptimal temperature and elevated O_3 concentration on the primary metabolism of leaf mustard are negative and stronger than their individual effects and (ii) supraoptimal temperatures worsen O_3 damage by regulating stomatal movement in *B. juncea*.

2. Materials and Methods

2.1. Plant Material and O_3 Fumigation Chamber

Seedlings of leaf mustard (*B. juncea*), which is widely cultivated in East Asia, were used as the test plant material in this study. Seeds were germinated and cultivated for 2 weeks in a closed-type plant factory (temperature: 20 ± 2 °C; relative humidity: 60 ± 5%; light intensity: 200 ± 20 mol m^{-2} s^{-1}; day length: 16 h) at the University of Seoul, Seoul, Korea (37°34′57.5″ N, 127°03′39.1″ E). Thereafter, the seedlings were transplanted into 3 L plastic pots filled with a growing medium containing perlite, vermiculite, and peat moss (Green Partner, Nongwoo Bio, Suwon, Korea). All test seedlings were allowed to acclimatize for a week in the chambers, which were enclosed by glass, under sunlight before starting the treatments.

The present experiment was performed in growth chambers (Growth chamber, Koito Industries, Yokohama, Japan) equipped with an O_3 generator (ON-1-2, Nippon Ozone Co., Tokyo, Japan). The fumigation system has been described elsewhere [39]. For each test, 15 plants with similar growth conditions were placed in a control chamber with a charcoal filter, and an additional 15 plants were placed in a treatment chamber with an O_3 fumigator. All plants were irrigated well and randomly placed everyday throughout the experiment. Leaves were sampled twice at 7 and 14 days after the beginning of exposure (DAE) between 09:00 and 12:00 h. The experiment lasted from March to April 2018. Fully expanded leaves were used to analyze the O_3 response of physiological and stomatal characteristics. Samples were stored at − 80 °C until analysis.

The treatment conditions in the growth chamber are summarized in Table 1. The elevated O_3 concentration used was based on the hourly average maximum O_3 concentration from March to July 2016 measured in South Korea [40]. The optimal temperature was 22 °C, since *Brassica* spp. grow the best within the temperature range of 22–25 °C according to previous reports [41–43]. The supraoptimal temperature was 5 °C above the optimal temperature range for leaf mustard considering one of the moderate scenarios for

2100 projected previously [3]. The test plants were exposed to O_3 for 8 h daily from 09.30 to 17.30 h while controlling the temperature and relative humidity for 24 h (Figure 1).

Table 1. Controlled environmental conditions in each treatment chamber in the experiment.

Treatment	Notation	Ozone Concentration (ppb)	Temperature (°C, Day/Night)
Charcoal-filtered O_3 + optimal temperature	C	11 ± 3.4	22/20
Charcoal-filtered O_3 + supraoptimal temperature	T	13 ± 3.9	27/25
Elevated O_3 + optimal temperature	O	105.6 ± 9.2	22/20
Elevated O_3 + supraoptimal temperature	OT	103 ± 9.9	27/25

Values are presented as mean ± SD (n = 5).

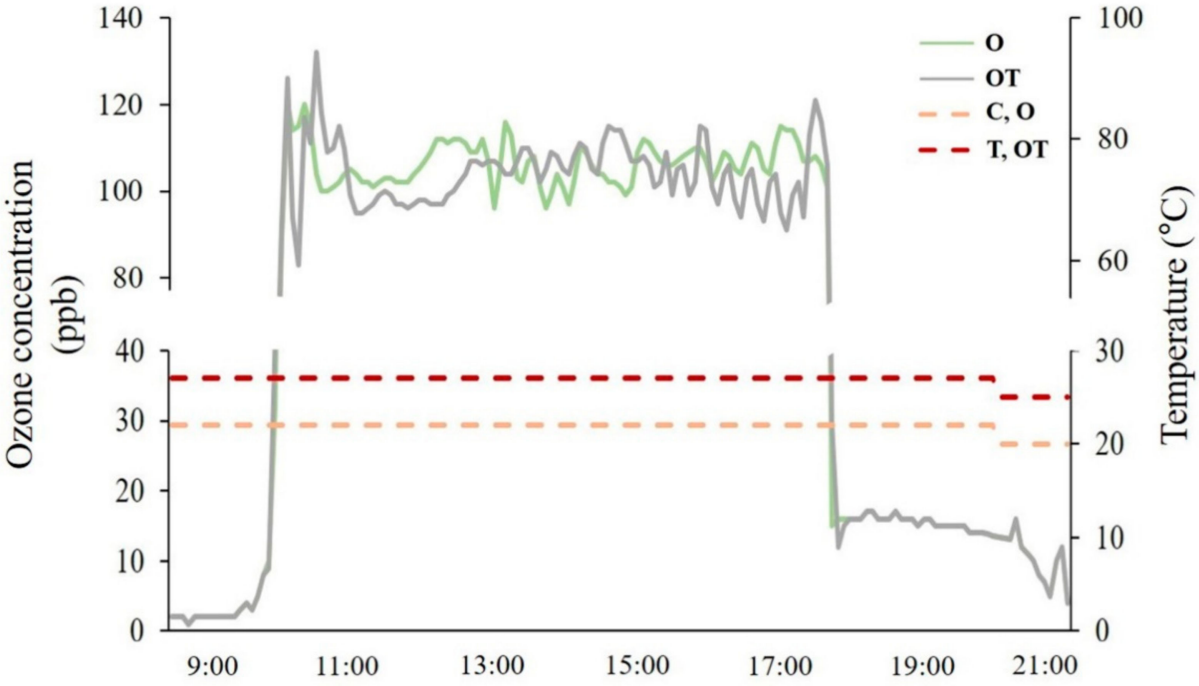


Figure 1. Daily variation in ozone concentration (solid line) and temperature (dash line) in each treatment chamber. C: optimal temperature + ambient O_3; T: supraoptimal temperature + ambient O_3; O: optimal temperature + elevated O_3; OT: supraoptimal temperature + elevated O_3.

2.2. Physiological Characteristics

Photosynthetic rate curves were plotted against intercellular CO_2 concentration (A/C_i) using a portable photosynthesis measurement system (Li-6400 XT, LI-COR Inc., Lincoln, NE, USA) with an LED source (6400-02B, LI-COR Inc., Lincoln, NE, USA). Measurements were performed on the second to fourth fully expanded leaves in each treatment group, with CO_2 concentration settings of 50, 100, 150, 200, 400, 600, 800, 1000, and 1200 µmol mol^{-1}, tested under photosynthetically active radiation of 1000 µmol m^{-2} s^{-1}, block temperature of 20 °C, and relative humidity of 50–60%. The maximum reaction velocity of RuBisCO for carboxylation (V_{cmax}), maximum rate of electron transport (J_{max}), triose phosphate use (TPU), daytime respiration (R_d), and mesophyll conductance (g_m) were calculated based on the response curves using the A/C_i curve fitting utility program described previously [44].

Chlorophyll *a* (Chl *a*) fluorescence was determined for the second to fourth fully developed leaves using Pocket PEA software (PEA plus V1.10, Hansatech Instrument Ltd., Norfolk, UK) between 10.00 and 12.00 h. Before measurement, leaves were adapted to darkness using leaf clips for 30 min. A saturating pulse at an intensity of 3500 µmol

m^{-2} s^{-1} (peak wavelength, 627 nm) was applied to the upper surface of the test leaves to measure the minimum fluorescence (F_o), maximum fluorescence (F_m), and OJIP transients. The maximum photochemical efficiency of photosystem II (PS II) was determined as the ratio of variable fluorescence ($F_v = F_m - F_o$) to maximum fluorescence (F_v/F_m).

The measured values of OJIP transients indicate F_o intensity at 50 µs when all PS II reaction centers (RCs) are open (O-step), fluorescence intensity at 2 ms (J-step), fluorescence intensity at 30 ms (I-step), and F_m intensity when all PS II RCs are closed (P-step). The JIP parameters were calculated to identify the extent of damage to the electron acceptor sites of PS II by O_3 according to the JIP test equations [45,46]. The value of each JIP parameter is listed in Table S1.

2.3. Chlorophyll Content

Chl *a*, chlorophyll b (Chl *b*), and total chlorophyll (Chl *a* + Chl *b*) content was estimated as previously described [47]. Fresh leaves (0.1 g) were extracted in 10 mL of 80% (*v*/*v*) acetone for 14 days at 4 °C. The chlorophyll content was quantified using a microplate reader (Epoch Microplate Spectrophotometer, Synergy, BioTek, Winooski, VT, USA) at an absorbance (*A*) of 663, 645, and 470 nm. Chlorophyll content was determined using the following formulas:

$$\begin{aligned} \text{Chlorophyll a (mg g}^{-1}\text{ FW)} &= 12.7 \times A_{663} - 2.69 \times A_{645} \\ \text{Chlorophyll b (mg g}^{-1}\text{ FW)} &= 22.9 \times A_{645} - 4.68 \times A_{663} \\ \text{Total chlorophyll (mg g}^{-1}\text{ FW)} &= 20.2 \times A_{645} + 8.02 \times A_{663}. \end{aligned} \quad (1)$$

In practice, the phytol chain of chlorophyll molecules can be easily cleaved with the addition of 80% acetone [48]. We did not consider the phytol chain cleavage, because phytol has the same absorption and light spectra as chlorophyll and thus does not affect the values obtained using this method [49].

2.4. Stomatal Characteristics

For the measurement of stomatal characteristics, leaf samples were harvested at 14 DAE between 09:00 and 12:00 h and freeze-dried using a lyophilizer (FD 8508, ilShinbiobase CO. Ltd., Dongducheon, South Korea). Stomatal density per leaf and stomatal size were evaluated via field emission scanning electron microscopy (FESEM; SU-70, Hitachi, Tokyo, Japan). Stomatal density was determined based on the number of stomata obtained by FESEM.

2.5. Hydrogen Peroxide (H_2O_2) and Superoxide (O_2^-) Accumulation

H_2O_2 and O_2^- accumulation in sampled leaves was measured as described previously [50], with slight modification. To detect H_2O_2, leaf discs were cut with a cork borer (diameter, 2 cm), vacuum-infiltrated in 1 mg ml^{-1} of 3,3-diaminobenzidine (DAB) in 0.2 M HCl (pH 3.8), and incubated at 25 °C for 4 h in the dark. To detect O_2^-, the leaf discs were cut (diameter, 2 cm), vacuum-infiltrated in 50 mM potassium phosphate buffer (pH 7.8) containing 0.1% (*w*/*v*) nitroblue tetrazolium (NBT), and incubated at 25 °C for 20 min in the dark. For both measurements, leaf discs were immersed in 96% (*v*/*v*) ethanol for 20 min at 70 °C to remove chlorophyll. After cooling, the leaf discs were stored in 70% (*v*/*v*) glycerol. The leaf discs were photographed and observed under a stereomicroscope (Leica M275, Leica Microsystems, Mannheim, Germany). The stained areas were calculated as the proportion of pixels in the stained area to the total pixels using Adobe Photoshop CS6 (Adobe Inc., Mountain View, CA, USA).

2.6. Growth Characteristics

All plants in each treatment chamber were collected at 14 DAE. Five plants per treatment were randomly selected to determine leaf fresh and dry weight, leaf number, and leaf area. Leaf area was measured on three fully expanded leaves of five plants using

winFolia (Regent Instruments Inc., Sainte-Foy, QC, Canada). Leaf dry weight was obtained by drying the samples for 48 h at 60 °C in an oven (HK-300DO, HUKO FS, Seoul, Korea).

2.7. Statistical Analysis

Effects of O_3 concentration, temperature, sampling date, and their interactions on the physiological and stomatal characteristics of *B. juncea* were analyzed using two-way or three-way analysis of variance (ANOVA). Tukey's honestly significant difference test ($p \leq 0.05$) was used to compare the differences among the parameters tested. Significance of differences in values at 7 and 14 DAE among various treatments was tested using independent *t*-test. All analyses were performed using SPSS Statistics 25 (SPSS Inc., Chicago, IL, USA). Values in figures and tables are presented as mean ± SD.

3. Results

3.1. A/C_i Curve Response

At 7 DAE, V_{cmax} was significantly decreased under ambient O_3 + supraoptimal temperature (T) (by 19.3%) and elevated O_3 + supraoptimal temperature (OT) (by 36.2%) conditions compared with that under ambient O_3 + optimal temperature (C) conditions. At 14 DAE, V_{cmax} under O and OT conditions was significantly reduced by respectively 44.6% and 54.3% compared with that under C conditions. Therefore, supraoptimal temperatures did not significantly affect the V_{cmax} of *B. juncea* at 14 DAE (Figure 2). Three-way ANOVA showed that V_{cmax} was significantly affected by all individual factors and their interactions except for the temperature × O_3 × sampling date interaction (Table S2).

At 7 and 14 DAE, J_{max} under OT conditions was significantly decreased by respectively 34.9% and 67.9% compared with that under C conditions. Furthermore, J_{max} under O conditions was significantly reduced by 55.05% compared with that under C conditions (Figure 2). Three-way ANOVA showed that two individual factors, namely elevated O_3 and sampling date, significantly affected J_{max}. Moreover, the interactions among factors also significantly affected J_{max}, except the temperature × O_3 × sampling date interaction (Table S2).

At 7 DAE, there were no significant differences in TPU under O, OT, and T conditions compared with that under C conditions; however, at 14 DAE, TPU under O (by 31.6%) and OT (by 43.4%) conditions was significantly reduced compared with that under C conditions (Figure 2). Three-way ANOVA showed that TPU was significantly affected by two individual factors, namely elevated O_3 and sampling date, as well as by interactions among all factors, except the temperature × O_3 × sampling date interaction (Table S1).

At 7 DAE, R_d was increased under OT conditions compared with that under C and O conditions (by 56.3% and 53.3%, respectively). At 14 DAE, R_d under T conditions was significantly increased (by 44.8%) compared with that under C conditions (Figure 3). Three-way ANOVA showed that elevated temperature strongly affected R_d (Table S2).

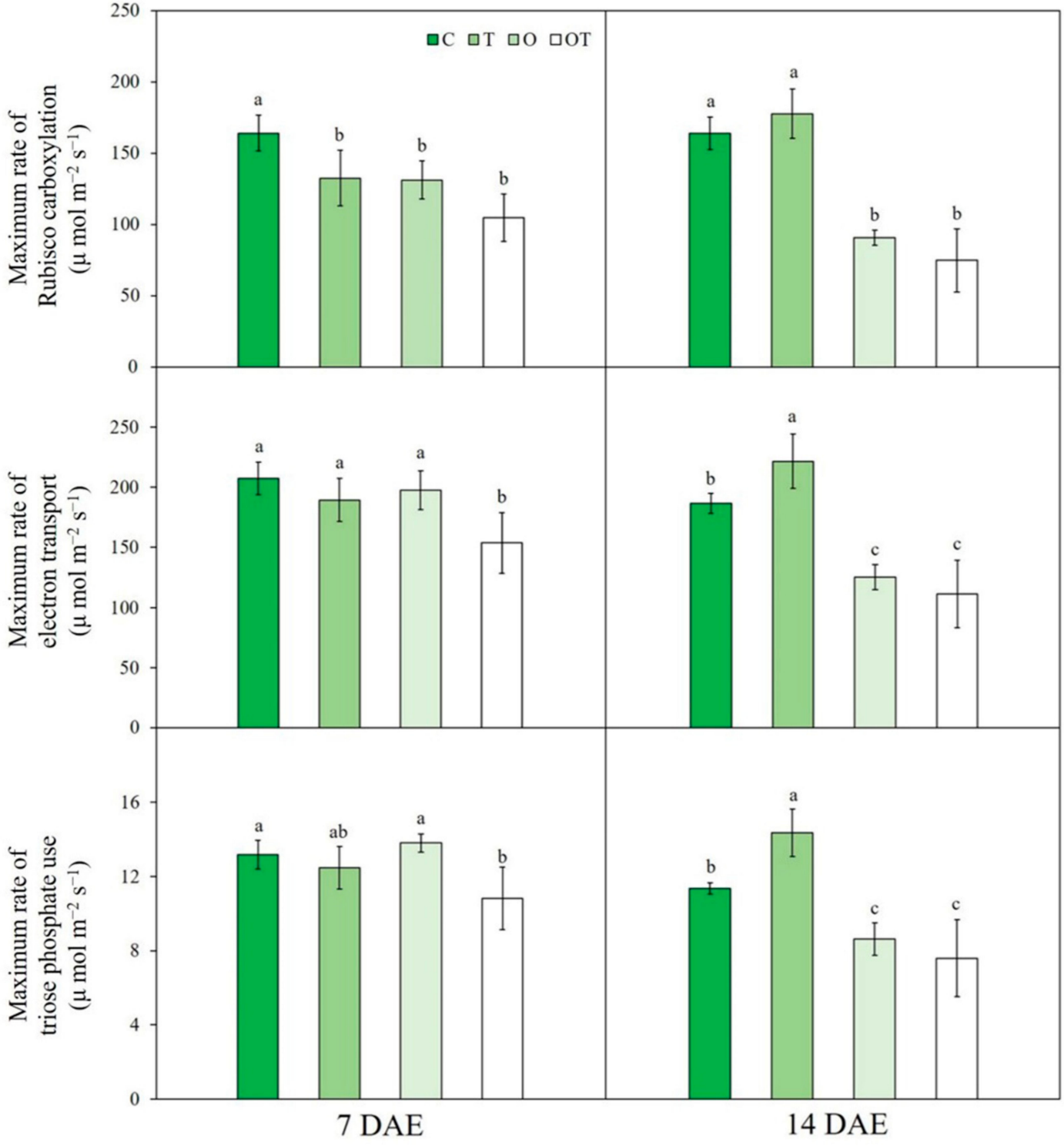


Figure 2. The maximum rate of ribulose 1,5-bisphosphate carboxylase/oxygenase (RuBisCo) carboxylation, electron transport, and triose phosphate use of *Brassica juncea* L. under different ambient and supraoptimal temperatures and O_3 concentrations at 7 and 14 DAE. Data are plotted as mean ± SD (n = 5). Different letters indicate significant differences among treatments at $p < 0.05$ according to Tukey's honestly significant difference test. C: ambient O_3 + optimal temperature; T: ambient O_3 + supraoptimal temperature; O: elevated O_3 + optimal temperature; OT: elevated O_3 + supraoptimal temperature; DAE: days after the beginning of exposure.

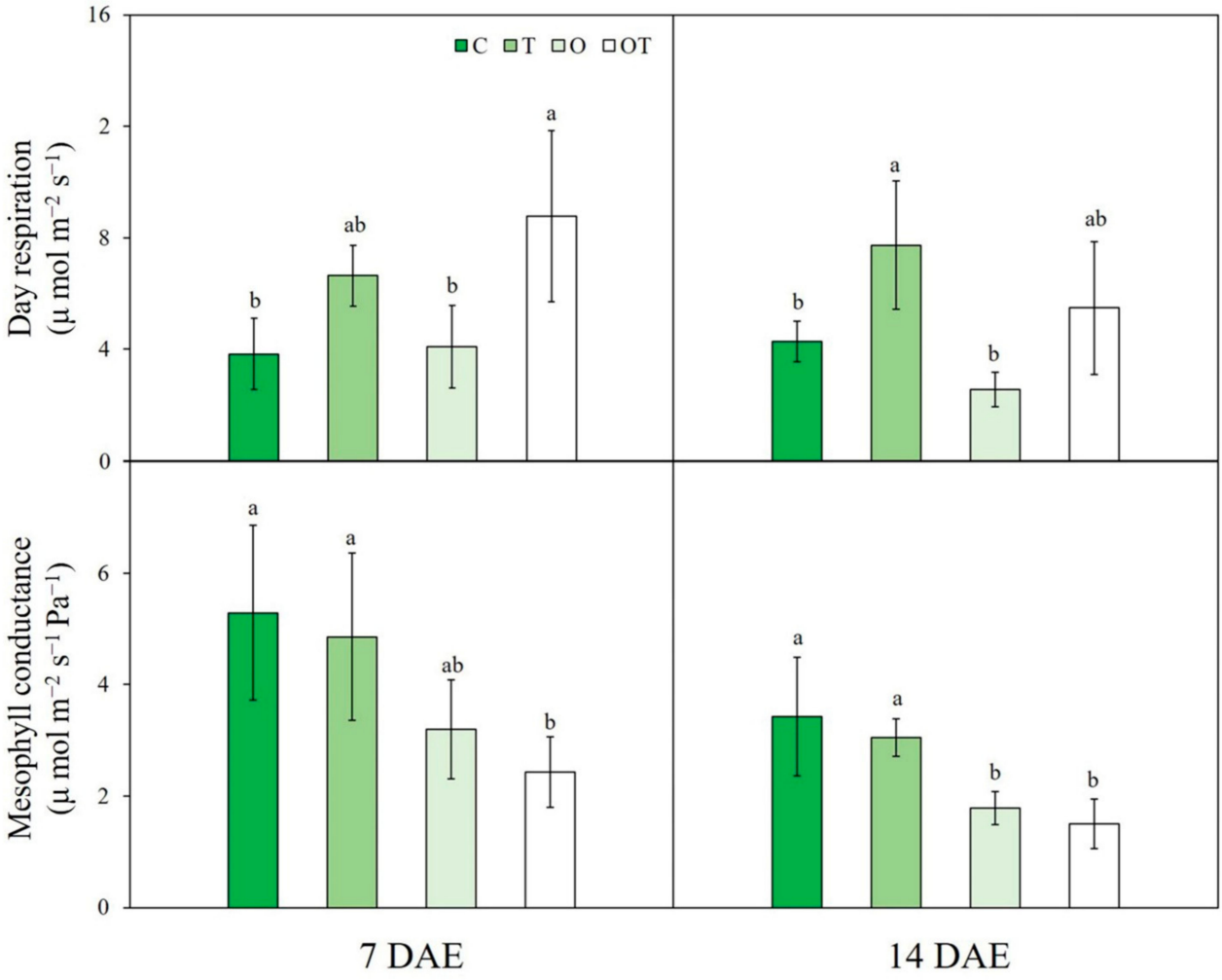


Figure 3. Daytime respiration and mesophyll conductance of *Brassica juncea* L. under different ambient and supraoptimal temperatures and O_3 concentrations at 7 and 14 DAE. Data are plotted as mean ± SD (n = 5). Different letters indicate significant differences among treatments at $p < 0.05$ according to Tukey's honestly significant difference test. C: ambient O_3 + optimal temperature; T: ambient O_3 + supraoptimal temperature; O: elevated O_3 + optimal temperature; OT: elevated O_3 + supraoptimal temperature; DAE: days after the beginning of exposure.

Moreover, g_m was significantly reduced under OT conditions compared with that under C conditions. Similarly, g_m under OT conditions was significantly reduced by 47.4% compared with that under T conditions (Figure 3). Three-way ANOVA indicated that g_m was significantly affected by the sampling date alone (Table S2).

3.2. Chl Content

At 14 DAE, total Chl content was significantly decreased under O (by 23.2%) and OT (by 55.3%) conditions compared with that under C conditions. However, at 7 DAE, total Chl content was significantly reduced under OT (by 36.2%) conditions alone (Figure 4). Total Chl content was affected by two individual factors, namely supraoptimal temperature and O_3, whereas sampling date and interactions among all factors did not significantly affect total Chl content, except the O_3 × sampling date interaction (Table S2).

Chl a/b ratio was significantly reduced under OT conditions compared with that under C conditions at both 7 (by 25.0%) and 14 (by 25.7%) DAE (Figure 4). Three-way ANOVA showed no significant effect of any factor or interaction on this ratio except for the temperature × sampling date interaction (Table S2).

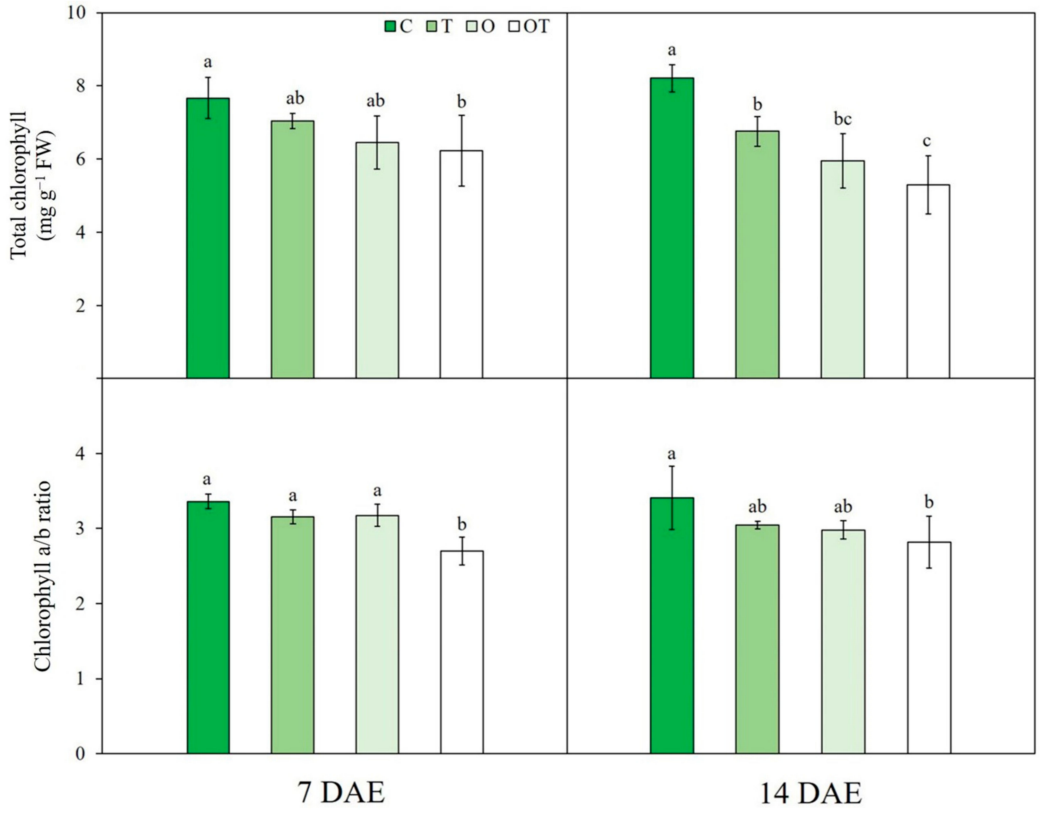


Figure 4. Total chlorophyll content and chlorophyll a/b ratio of *Brassica juncea* L. under different ambient and supraoptimal temperatures and O_3 concentrations at 7 and 14 DAE. Data are plotted as mean ± SD (n = 5). Different letters indicate significant differences among treatments at $p < 0.05$ according to Tukey's honestly significant difference test. C: ambient O_3 + optimal temperature; T: ambient O_3 + supraoptimal temperature; O: elevated O_3 + optimal temperature; OT: elevated O_3 + supraoptimal temperature; DAE: days after the beginning of exposure.

3.3. Chl a Fluorescence

In the OJIP transient curves of *B. juncea*, each step showed a different response to various treatments. Overall, the expected degradation of the photosynthetic apparatus in plants grown under O and OT conditions was observed in the OJIP transient curves. Fluorescence at the J-step was significantly reduced under OT conditions compared with that under C conditions at 7 and 14 DAE (by 12% and 23.7%, respectively). Fluorescence at the I-step was also significantly decreased under OT conditions compared with that under C conditions at 14 DAE (by 28.8%). Moreover, relative fluorescence at the P-step was decreased under O and OT conditions (by 25% and 33%, respectively) compared with that under C conditions at 14 DAE (Figure 5B). The values of JIP parameters estimated based on the OJIP transient curves of Chl *a* fluorescence were significantly different between the test and controls plants, and these values were used to construct the spider plots shown in Figure 6. There were no significant differences among treatments in terms of phenomenological fluxes per excited cross-section (CS) at both 7 and 14 DAE. The maximum quantum yield of PS II (φP_O) was significantly decreased, but the quantum yield of energy dissipation (φD_O), electron transport flux per RC (ET_O/RC), and dissipated energy flux per RC (DI_O/RC) were significantly increased under OT conditions compared with that under C conditions at 7 DAE. The absorption flux, trapped energy flux, and electron transport flux per RC under O conditions were significantly increased compared with those under C conditions at 7 DAE. Compared with controls, test plants showed significantly reduced φP_O, Q_A reducing PS II RC/CS, and performance index assessed on an absorption basis (PI_{ABS}) but significantly increased φD_O, ET_O/RC, and DI_O/RC under

both O and OT conditions at 7 DAE. The estimated initial slope of the fluorescence transient (Mo), relative variable fluorescence at 2 ms (V_J), absorption flux per RC (ABS/RC), and trapped energy flux per RC (ET_O/RC) were significantly increased under O conditions compared with those under C conditions at 14 DAE (Figure 6).

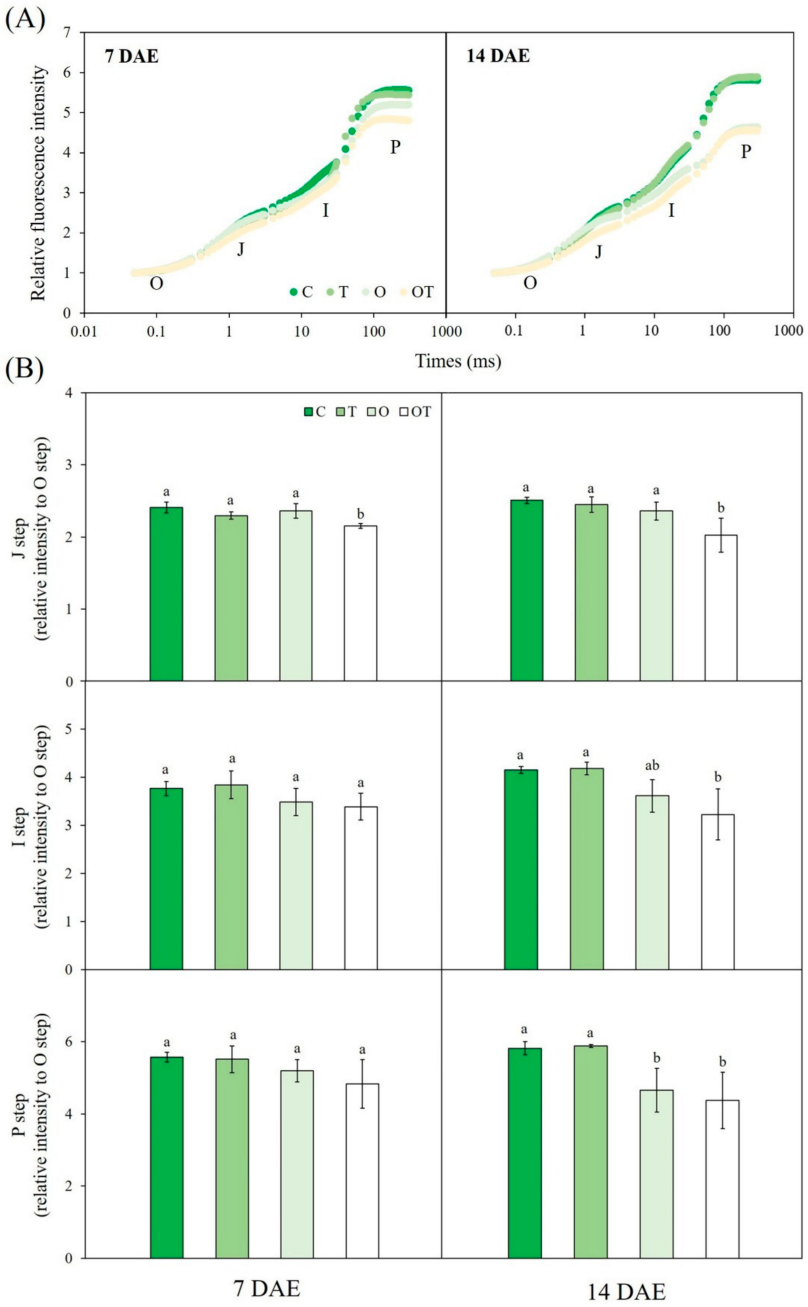


Figure 5. (**A**) Chlorophyll *a* fluorescence OJIP transient curves and (**B**) J-, I-, and P-steps derived from chlorophyll *a* fluorescence OJIP transient curves of *Brassica juncea* L. under different ambient and supraoptimal temperatures and O_3 concentrations at 7 and 14 DAE. The J- (intensity at 2 ms), I- (intensity at 30 ms), and P (maximum intensity when all PS II reaction centers (RCs) are closed) steps in the figure indicate fluorescence intensity at these points relative to that at the O-step (when all PS II RCs are open). Data are plotted as mean ± SD (n = 5). Different letters indicate significant differences among treatments at $p < 0.05$ according to Tukey's honestly significant difference test. C: ambient O_3 + optimal temperature; T: ambient O_3 + supraoptimal temperature; O: elevated O_3 + optimal temperature; OT: elevated O_3 + supraoptimal temperature; DAE: days after the beginning of exposure.

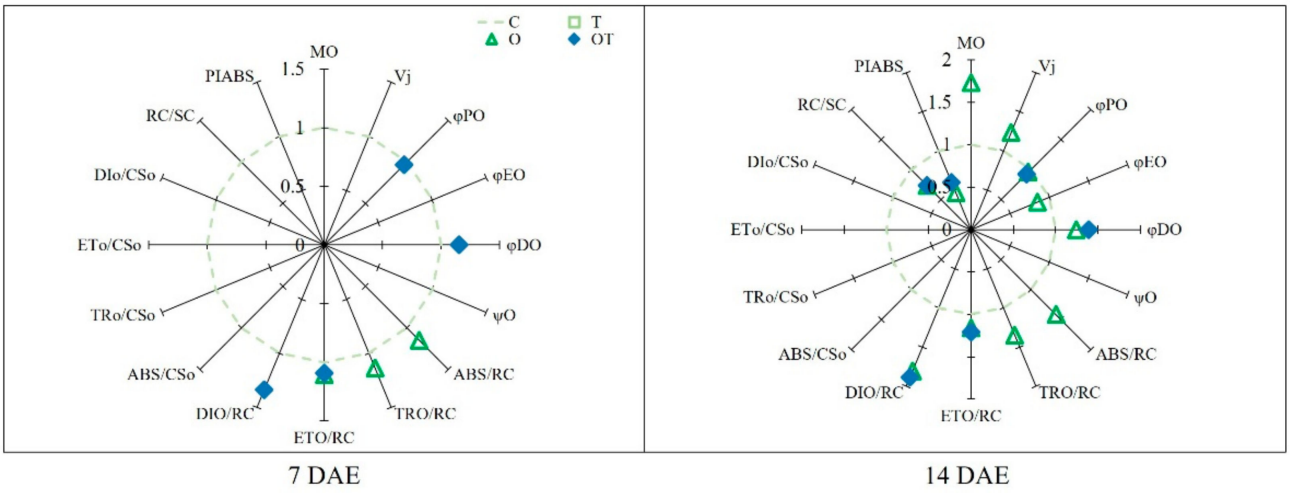


Figure 6. Spider plots of JIP parameters derived from chlorophyll *a* fluorescence OJIP transient curves of *Brassica juncea* L (see Table S1 for definitions) under different ambient and supraoptimal temperatures and O_3 concentrations at 7 and 14 DAE. The parameters values of plants grown under control conditions were set to 1. Only parameter values that were significantly different from those under C conditions at $p < 0.05$ according to Tukey's honestly significant difference test are shown in the figure. C: ambient O_3 + optimal temperature; T: ambient O_3 + supraoptimal temperature; O: elevated O_3 + optimal temperature; OT: elevated O_3 + supraoptimal temperature; DAE: days after the beginning of exposure.

3.4. Stomatal Characteristics

The stomatal appearance differed among plants exposed to supraoptimal temperature, elevated O_3 concentration, or a combination of both (Figure 7A). Stomatal density on the abaxial leaf surface in *B. juncea* was decreased (by 45%) under O conditions compared with that under C conditions. However, there were no significant differences in stomatal density under T, OT, and C conditions (Figure 7B). The stomatal pore area was slightly increased by supraoptimal temperatures, albeit not significantly. The stomatal pore area was significantly decreased under O (by 57.8%) and OT (53.9%) conditions compared with that under C conditions (Figure 7B). Two-way ANOVA showed that individual factors and their interactions significantly affected stomatal density, whereas only ambient and elevated O_3 concentration significantly affected stomatal pore area (Table S2).

3.5. H_2O_2 and O_2^- Accumulation

DAB and NBT staining showed ROS accumulation in *B. juncea* at 14 DAE (Figure 8A). The DAB-stained area, representing H_2O_2 accumulation, was significantly increased under O and OT conditions compared with that under C conditions. However, there were no significant differences between C and T conditions at 14 DAE (Figure 8B). In addition, there were no significant differences between O and OT conditions. Following NBT staining at 14 DAE, blue spots indicating O_2^- accumulation were the most abundant under OT conditions (Figure 8A). NBT staining revealed O_2^- accumulation in the leaves of plants under O and OT conditions at 14 DAE. Blue spots resulting from a reaction between O_2^- and NBT were the most abundant in the leaves of plants under OT conditions (Figure 8B). Two-way ANOVA showed that all individual factors, but not their interactions, significantly affected H_2O_2 accumulation. Moreover, all individual factors and their interactions significantly affected O_2^- accumulation (Table S2).

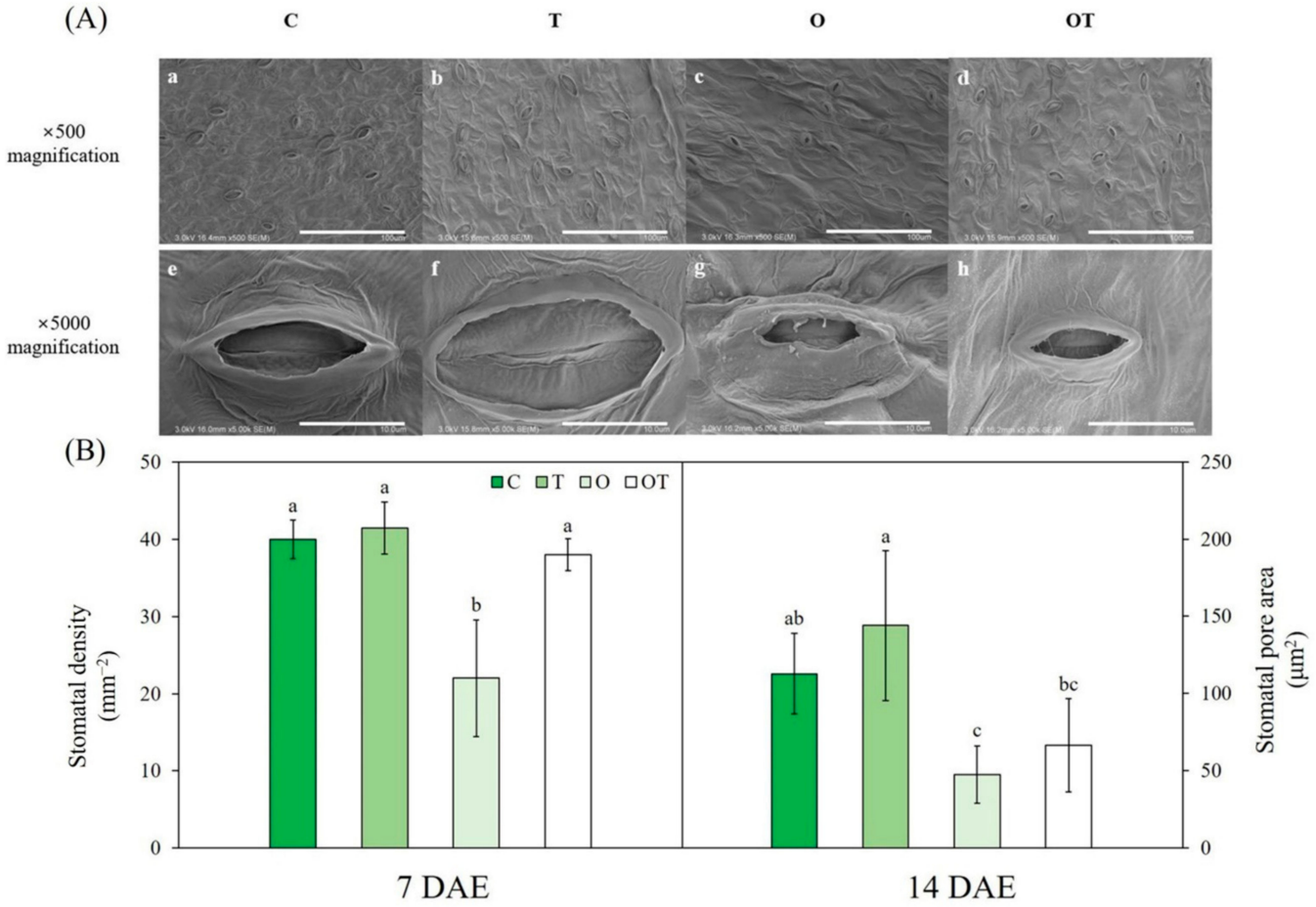


Figure 7. (**A**) Field emission scanning electron micrographs (A–H) and (**B**) stomatal density and stomatal pore area of *Brassica juncea* L. under different ambient and supraoptimal temperatures and O_3 concentrations at 14 DAE. Micrographs under control conditions (A,E); at supraoptimal temperature and ambient O_3 (B,F); at optimal temperature and elevated O_3 (C,F); and at supraoptimal temperature and elevated O_3 (D,H) at 500 and 5000× magnification, respectively. (a–d) Scale bar = 100 μm. (e–h) Scale bar = 10 μm. Data are plotted as mean ± SD (n = 5). Different letters indicate significant differences among treatments at $p < 0.05$ according to Tukey's honestly significant difference test. C: ambient O_3 + optimal temperature; T: ambient O_3 + supraoptimal temperature; O: elevated O_3 + optimal temperature; OT: elevated O_3 + supraoptimal temperature; DAE: days after the beginning of exposure.

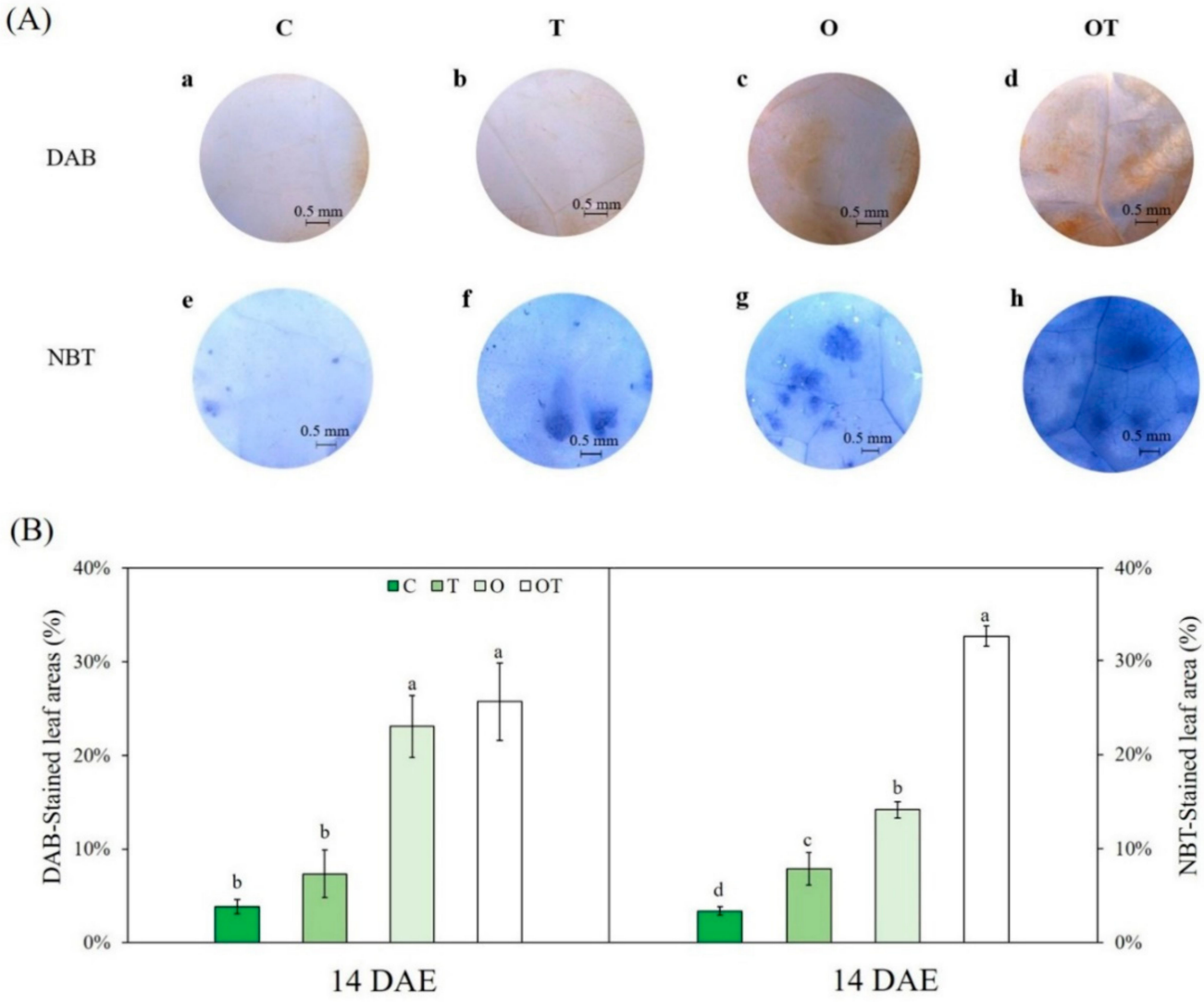


Figure 8. (**A**) Hydrogen peroxide (H_2O_2) and superoxide (O_2^-) accumulation and (**B**) percentage of 3,3′-diaminobenzidine (DAB)- and nitroblue tetrazolium (NBT)-stained leaf area of *Brassica juncea* L. under different ambient and supraoptimal temperatures and O_3 concentrations at 14 DAE. (a–d) Histochemical detection of H_2O_2 in *B. juncea* leaves by DAB staining. (e–h) Histochemical detection of O_2^- in *B. juncea* leaves by NBT staining. H_2O_2 and O_2^- accumulation under control conditions (a,e); at supraoptimal temperature and ambient O_3 (b,f); at optimal temperature and elevated O_3 (c,g); and at supraoptimal temperature and elevated O_3 (d,h) at 14 DAE. Scale bars = 0.5 mm. Data are plotted as mean ± SD (n = 5). Different letters indicate significant differences among treatments at $p < 0.05$ according to Tukey's honestly significant difference test. C: ambient O_3 + optimal temperature; T: ambient O_3 + supraoptimal temperature; O: elevated O_3 + optimal temperature; OT: elevated O_3 + supraoptimal temperature; DAE: days after the beginning of exposure.

3.6. Plant Growth Characteristics

Leaf fresh weight was significantly decreased under T, O, and OT (by 26.5%, 57.3%, and 93.4%, respectively) conditions compared with that under C conditions. Leaf fresh weight under OT conditions was significantly decreased compared with that under O conditions. Conversely, leaf dry weight was not significantly different between OT and O conditions (Figure 9). Leaf dry weight was significantly decreased under T, O, and OT (by 34.7%, 48.3%, and 55.8%, respectively) conditions compared with that under C conditions. Leaf number and area were significantly decreased under O and OT conditions compared with those under C conditions (Figure 9). However, there were no significant differences between O and OT conditions. Two-way ANOVA showed that leaf fresh and dry weight

was significantly affected by all individual factors and their interactions, whereas leaf number and area were not affected by any factor or interaction (Table S2).

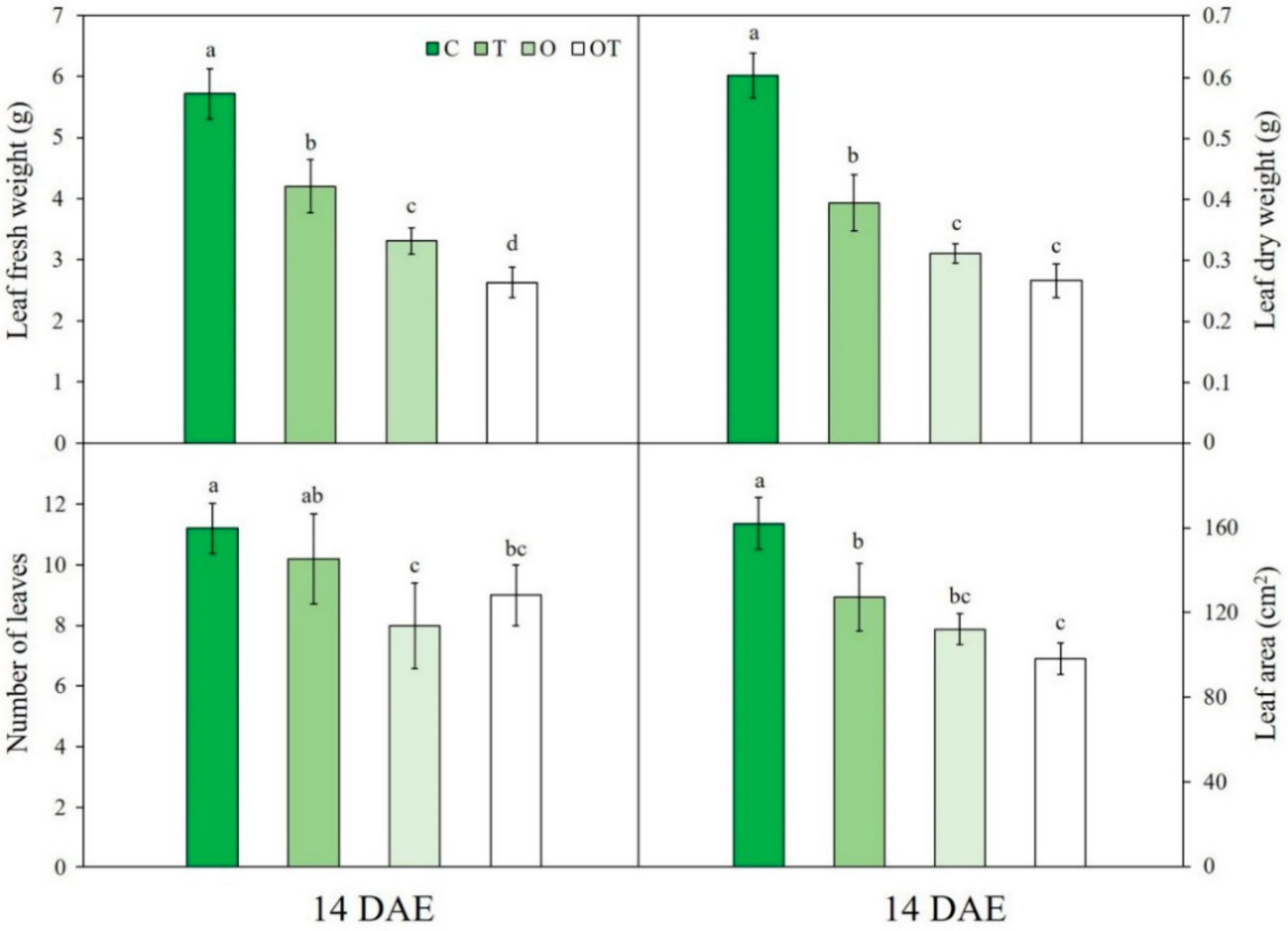


Figure 9. Leaf fresh weight, dry weight, number, and area of *Brassica juncea* L. under different ambient and supraoptimal temperatures and O_3 concentration at 14 DAE. Data are plotted as mean ± SD (n = 5). Different letters indicate significant differences among treatments at $p < 0.05$ according to Tukey's honestly significant difference test. C: ambient O_3 + optimal temperature; T: ambient O_3 + supraoptimal temperature; O: elevated O_3 + optimal temperature; OT: elevated O_3 + supraoptimal temperature; DAE: days after the beginning of exposure.

4. Discussion

Given the potential effects of supraoptimal temperature and elevated O_3 on plants, the present study explored the impact of these environmental factors on the physiological and stomatal characteristics of *B. juncea*. We demonstrated that the interactions of supraoptimal temperature and elevated O_3 negatively affected leaf mustard rather than the individual factors.

Regarding physiological characteristics, *B. juncea* leaves showed lower photosynthetic capacity under OT conditions than under other conditions, as indicated by V_{cmax}, J_{max}, and TPU. Measurements of V_{cmax} and J_{max}, which are indicators of biochemical capacity, are typically based on intercellular CO_2. V_{cmax} decreased under O and OT conditions compared with that under C conditions at both 7 and 14 DAE (Figure 2). This result is consistent with previous reports on the effects of O_3 on plant physiological characteristics [51,52]. Previous research found a significant reduction in net photosynthesis (P_n) of *B. juncea* under O and OT conditions compared to C at 7 and 14 DAE. Furthermore, there was also significant difference in P_n between O and OT conditions at 14 DAE [39]. V_{cmax} indicates the intrinsic photosynthetic capacity as well as RuBisCo activity and kinetics, and J_{max} indicates the

rate of RuBP regeneration via electron transport [44,53]. Biochemical limitations related to RuBisCo are associated with reduced CO_2 assimilation in the presence of elevated O_3 [54,55]. In general, O_3 reduces the RuBisCo protein content of plants by producing ethylene [56]. O_3 stress impairs the photosystems (PSs), thereby generating the energy required to produce NADPH (nicotinamide adenine dinucleotide phosphate) and ATP (adenosine triphosphate) [57]. Photosynthetic capacity is linked to leaf nitrogen (N) content since the majority of leaf N comes from thylakoid proteins and stromal enzymes [58]. O_3 can result in lower N content per leaf area, higher investment of N in cell walls, and a reduction of leaf N allocation to photosynthetic processes [59]. However, in the present study, there were no significant differences in V_{cmax} between C and T conditions at 14 DAE (Figure 2). This result suggests that supraoptimal temperature (5 °C above the optimal) did not affect V_{cmax} as much as elevated O_3 did. The same tendency was observed for J_{max} and TPU. Similarly, Thwe et al. [57] have reported a strong correlation between V_{cmax} and J_{max} in tomato under O_3 stress. However, some previous studies have reported that a minor limitation to RuBisCo activation is closely related to moderately high temperatures [60,61]. Indeed, in the present study, J_{max} and TPU were not significantly affected by supraoptimal temperatures alone (Table S2). Increased J_{max} and TPU were observed under T conditions compared with those under C conditions (Figure 2). By shifting the operating range beyond the optimal temperature, short-term supraoptimal temperature of about 5 °C may decrease P_n [62]. In previous study, P_n of *B. juncea* under elevated temperature was significantly decreased compare to that in optimum temperature at 7 DAE [39]. This form of acclimation, which results in a general up-regulation of leaf N and photosynthetic proteins, is based on the availability of N resources for higher investment in the photosynthetic apparatus [62]. Under sustained high temperatures, most plants can acclimate their photosynthetic traits. Through thermal acclimation, metabolic activities are modified to compensate for temperature changes, resulting in metabolic homeostasis [63]. Three-way ANOVA on the response parameters of A/Ci curves indicated that R_d was significantly affected by supraoptimal temperature. The rates of enzymatic processes involved in R_d are enhanced by high temperatures [64]. An increase in R_d along with a decrease in net photosynthesis reduces carbohydrate availability to plants [65]. In this study, there were no significant differences in these parameters in the presence of elevated O_3. Contrary to our results, Calatayud et al. [51] reported increased R_d in a Mediterranean endemic plant exposed to an O_3 concentration of 70 ppb. In this study, significant reductions in g_m were observed under O conditions at 14 DAE and under OT conditions at both 7 and 14 DAE compared with the values under C conditions (Figure 3). Several studies on soybean, birch, and poplar have reported negative effects of elevated O_3 on g_m [66–68]. As such, g_m is affected by O_3 conductance through cell wall, intercellular air spaces, and intracellular fluid [69]. Elevated O_3 likely reduces g_m via mechanisms involving the altered levels, shape, and position of the chloroplasts and thickening of the cell wall [70]. g_m is closely correlated with stomatal conductance (g_s), since CO_2 and H_2O are likely to share a common pathway in leaves [71]. In a previous study, a result was that a rapid transient decrease in g_s can occur when O_3 level was elevated as with g_m. The g_s of *B. juncea* under OT condition was found to be significantly lower than that of plants under T condition [39].

Reduced total Chl content is considered an indicator of O_3-induced biochemical damage [72]. In this study, total Chl content was decreased under O and OT conditions compared with that under C conditions at 14 DAE. Moreover, total Chl content under OT conditions was lower than that under T and O conditions at 14 DAE (Figure 4). A decrease in the total Chl content of leaves following O_3 exposure has been reported previously [73,74]. O_3 indirectly affects plant Chl content by accelerating leaf senescence [75]. A decrease in total Chl content generally reduces CO_2 assimilation [76], and there is a strong correlation between total Chl content and photosynthetic rate [77].

A significant decrease in the Chl a/b ratio was observed under OT conditions compared with that under C conditions at 7 and 14 DAE (Figure 4). These results regarding

the relative O_3 sensitivities of Chl *a* and *b* are overall contrary to previous reports [78]. There was a positive correlation between the ratio of Chl *a* to *b* and the ratio of PS II to light-harvesting chlorophyll *a*/*b* protein complex-II (LHCII) level. LHCII is the major light-harvesting complex in plants that exclusively contains Chl *b* and, accordingly, has a low Chl *a*/*b* ratio [79]. Czuba and Ormrod [80] reported that the Chl *b* content of *Lepidium sativum* L. was decreased to a greater extent than its Chl *a* content by O_3. However, greater reductions in Chl *a* content than in Chl *b* content by O_3 have also been reported in other plants [81].

In this study, OJIP transient curves were plotted and compared as indicators of photoinhibition in leaves under all treatments. Photoinhibition decreases the photosynthetic activity by reducing light-induced carbon assimilation [82]. Overall, the slope of OJIP curve significantly decreased from the J- to P-step under OT conditions at 7 and 14 DAE, whereas this decrease was only observed from the I- to P-step at 14 DAE (Figure 5A). These results indicate that the function of PS II RCs was more severely inhibited under OT conditions than under O conditions. Marzuoli et al. [83] reported that elevated O_3 levels significantly decreased PS II photochemical efficiency and electron flow in lettuce. O_3 induced ROS damage PS II RCs [84]. According to the OJIP transient curves in this study, elevated temperature did not negatively affect PS II RCs. However, φP_O was significantly decreased under OT conditions at both 7 and 14 DAE (Figure 6). This result is consistent with previous reports on the effects of elevated O_3 [57,85]. The observed φP_O reduction may be a result of enhanced non-photochemical processes of PS II light-harvesting antennae, which are related to the suppression of photochemical quenching and photodamage of PS II RCs [86]. In addition, φD_O was increased under O and OT conditions at 7 and 14 DAE (Figure 6). The observed increase in φD_O ($\varphi D_O = F_o/F_m$) was reflected in the increased value of F_o, which was perhaps due to the inactivation of some PS II RCs [87].

Stomata play a crucial role in determining the O_3 influx to leaves, because the majority of the O_3 enters the leaf via stomatal pores [88]. Since O_3 enters leaves of the plant through stomata, O_3 influx are highly dependent on stomatal density and conductance [89]. At 7 DAE, O_3 influx of *B. juncea* under OT condition was significantly higher than plants grown under O condition, as g_s significantly increased under OT compared to those in O [39]. Elevated O_3-induced oxidative stress also results in ultrastructural changes to mesophyll cells and their cell walls in plants, limiting O_3 entering into the leaves [90]. In a previous study, 100 ppb of O_3 led to the collapse of some epidermal cells adjacent to the stomata, and 150 ppb of O_3 led to the complete collapse of epidermal cells and loss of leaf structural integrity [91]. Consistent with previous reports, we observed a collapse of stomatal shape under O conditions (Figure 7A). Moreover, the stomatal density in leaf mustard under O conditions was significantly lower than that under other conditions at 14 DAE (Figure 7B). Neufeld et al. [92] reported that 100 ppb of O_3 tended to reduce stomatal density, suggesting structural changes in plants. Reductions in stomatal width and pore area in the presence of elevated O_3 have been confirmed in previous studies [93,94]. The stomatal density of *B. juncea* was affected by supraoptimal temperatures, elevated O_3, and their interaction, while its stomatal pore area was only affected by elevated O_3 (Table S2). Some previous studies have reported increased stomatal densities at supraoptimal temperatures [95,96]. Some plant species can develop leaves with different stomatal density in supraoptimal temperature, which can affect g_s [97]. g_s of *B. jnucea* under T and OT condition was significantly higher that in the C and O condition at 7 DAE, respectively. However, no significant difference in g_s between C and T condition was observed at 14 DAE, which was consistent with the result of stomatal density of *B. juncea* at 14 DAE [39].

Furthermore, increased H_2O_2 and O_2^- accumulation observed under O and OT conditions in this study suggests O_3 injury in *B. juncea* grown under these conditions. The visible injury of O_3 (necrosis and chlorosis) was observed on the leaves of plants grown under O and OT at both 7 and 14 DAE (Figure S1). The first O_3 injury symptoms on the surface of leaves under OT conditions at 3 DAE and those under O at 5 DAE were reported [39]. A major effect of O_3 on plants is ROS generation. ROS production in plant cells is closely

related to the O_3 flux and oxidative stress tolerance of plants [98,99]. ROS production is a critically harmful process and is also a key component of the abiotic stress responsive signaling networks of plants [100]. In this study, DAB and NBT staining indicated significant H_2O_2 and O_2^- accumulation, respectively, as a consequence of elevated O_3 (Table S2). These results indicate that long-term exposure to elevated O_3 can augment H_2O_2 and O_2^- production. Furthermore, our results showed an interactive effect of elevated O_3 and supraoptimal temperature on O_2^- accumulation, but not on H_2O_2 accumulation, in plant cells. O_2^- produces a strong effect on carbon assimilation, and it is a vital precursor of other ROS as an unstable radical with a high redox potential [101]. H_2O_2 can be produced from O_2^- via Mn-SOD [102].

In this study, we focused on the leaf growth response of *B. juncea*, because it is one of the most widely consumed leafy vegetables in East Asia. A significant decrease in leaf fresh and dry weight under O and OT conditions was observed (Figure 9). Many studies have indicated that prolonged O_3 exposure is typically detrimental to leaf growth and development [103], which is possibly due to O_3-induced damage to mesophyll cells upon uptake into the plants [104]. Li et al. [19] reported that the growth of eggplant (*Solanum melongena* L.) was significantly reduced in the presence of elevated O_3. Cell death as well as suppression of photosynthetic and stomatal activity in leaves can decrease the biomass and yield of leafy vegetables [105]. Additionally, leaf area was significantly reduced under O and OT conditions (Figure 9). The suppression of leaf primary metabolism leads to a reduction in leaf area [18].

5. Conclusions

By studying the responses of leaf physiological and stomatal characteristics, we demonstrated that elevated O_3 caused more severe damage in leaf mustard (*B. juncea*) at supraoptimal temperatures than at optimal temperatures. Stomatal density, which is related to O_3 influx to leaves, was higher in the presence of elevated O_3 at supraoptimal temperatures than that at optimal temperature, indicating detrimental effects of O_3 on the physiological, biochemical, and growth characteristics of *B. juncea* at 14 DAE. In particular, the interactive effects of O_3 stress and supraoptimal temperature decreased photosynthetic parameters, including J_{max} and TPU. Furthermore, Chl *a* fluorescence at the J-step of the OJIP transient curves was decreased in the presence of elevated O_3 at supraoptimal temperatures. Regarding biochemical characteristics, NBT-stained spots indicating O_2^- accumulation in plant cells were abundant under OT conditions. As a consequence of physiological and biochemical responses, elevated O_3 at supraoptimal temperatures significantly reduced leaf fresh and dry weight. Collectively, these findings indicate the interactions of supraoptimal temperature and elevated O_3 worsen the damage to *B. juncea* rather than the individual factors.

Supplementary Materials: The following are available online at https://www.mdpi.com/article/10.3390/land10040357/s1, Table S1: Formulas and descriptions of OJIP parameters based on data obtained from OJIP transient curves. Table S2: Results of analyses of variance of the main effects of temperature, O_3, and sampling date and their interactions on A/C_i curve response, chlorophyll content, chlorophyll *a* fluorescence, stomatal density, stomatal pore area, hydrogen peroxide and superoxide radical accumulation, and leaf growth parameters. Table S3: Comparison of each parameter under different ambient and supraoptimal temperatures and O_3 concentrations at 7 and 14 days after the beginning of exposure (DAE). Figure S1: Visible ozone symptoms of *Brassica juncea* L. under different optimal and supraoptimal temperatures and O_3 concentration at 7 and 14 DAE.

Author Contributions: S.Y.W. as the corresponding author, developed the concept, edited the manuscript, supervised the study, and acquired funding. J.K.L. designed the experiments, analyzed the data, and wrote the manuscript. M.J.K. and J.K.L. developed the analytical methods. H.D.K., S.H.P., Y.J.L., and S.G.J. organized the data input and analysis. M.J.K. and Y.S.C. edited the manuscript. All authors have read and agreed to the published version of the manuscript.

Funding: This work was supported by the Basic Study and Interdisciplinary R&D Foundation Fund of the University of Seoul (2019).

Institutional Review Board Statement: Not applicable.

Informed Consent Statement: Not applicable.

Data Availability Statement: Not applicable.

Conflicts of Interest: The authors declare no conflict of interest.

References

1. Tai, A.P.K.; Martin, M.V.; Heald, C.L. Threat to future global food security from climate change and ozone air pollution. *Nat. Clim. Chang.* **2014**, *4*, 817–821. [CrossRef]
2. Battisti, D.S.; Naylor, R.L. Historical warnings of future food insecurity with unprecedented seasonal heat. *Science* **2009**, *323*, 240–244. [CrossRef]
3. Pachauri, R.K.; Allen, M.R.; Barros, V.R.; Broome, J.; Cramer, W.; Christ, R.; Church, J.A.; Clarke, L.; Dahe, Q.; Dasgupta, P. *Climate Change 2014: Synthesis Report. Contribution of Working Groups I, II and III to the Fifth Assessment Report of the Intergovernmental Panel on Climate Change*; IPCC: Geneva, Switzerland, 2014.
4. Ainsworth, E.A. Rice production in a changing climate: A meta-analysis of responses to elevated carbon dioxide and elevated ozone concentration. *Glob. Chang. Biol.* **2008**, *14*, 1642–1650. [CrossRef]
5. Bita, C.E.; Gerats, T. Plant tolerance to high temperature in a changing environment: Scientific fundamentals and production of heat stress-tolerant crops. *Front. Plant Sci.* **2013**, *4*, 273. [CrossRef]
6. Zhao, C.; Liu, B.; Piao, S.; Wang, X.; Lobell, D.B.; Huang, Y.; Huang, M.; Yao, Y.; Bassu, S.; Ciais, P.; et al. Temperature increase reduces global yields of major crops in four independent estimates. *Proc. Natl. Acad. Sci. USA* **2017**, *114*, 9326–9331. [CrossRef] [PubMed]
7. DaMatta, F.M.; Grandis, A.; Arenque, B.C.; Buckeridge, M.S. Impacts of climate changes on crop physiology and food quality. *Food Res. Int.* **2010**, *43*, 1814–1823. [CrossRef]
8. Dusenge, M.E.; Duarte, A.G.; Way, D.A. Plant carbon metabolism and climate change: Elevated CO_2 and temperature impacts on photosynthesis, photorespiration and respiration. *New Phytol.* **2019**, *221*, 32–49. [CrossRef]
9. Fahad, S.; Bajwa, A.A.; Nazir, U.; Anjum, S.A.; Farooq, A.; Zohaib, A.; Sadia, S.; Nasim, W.; Adkins, S.; Saud, S.; et al. Crop production under drought and heat stress: Plant responses and management options. *Front. Plant Sci.* **2017**, *8*, 1147. [CrossRef]
10. Lawson, T.; Matthews, J. Guard Cell Metabolism and Stomatal Function. *Annu. Rev. Plant Biol.* **2020**, *71*, 273–302. [CrossRef] [PubMed]
11. Schlesinger, W.H.; Jasechko, S. Transpiration in the global water cycle. *Agric. For. Meteorol.* **2014**, *189–190*, 115–117. [CrossRef]
12. Urban, J.; Ingwers, M.W.; McGuire, M.A.; Teskey, R.O. Increase in leaf temperature opens stomata and decouples net photosynthesis from stomatal conductance in *Pinus taeda* and *Populus deltoides x nigra*. *J. Exp. Bot.* **2017**, *68*, 1757–1767. [CrossRef] [PubMed]
13. Zhang, H.; Pan, C.; Gu, S.; Ma, Q.; Zhang, Y.; Li, X.; Shi, K. Stomatal movements are involved in elevated CO_2 -mitigated high temperature stress in tomato. *Physiol. Plant.* **2019**, *165*, 569–583. [CrossRef]
14. Drake, J.E.; Tjoelker, M.G.; Vårhammar, A.; Medlyn, B.E.; Reich, P.B.; Leigh, A.; Pfautsch, S.; Blackman, C.J.; López, R.; Aspinwall, M.J.; et al. Trees tolerate an extreme heatwave via sustained transpirational cooling and increased leaf thermal tolerance. *Glob. Chang. Biol.* **2018**, *24*, 2390–2402. [CrossRef] [PubMed]
15. Duursma, R.A.; Blackman, C.J.; Lopéz, R.; Martin-StPaul, N.K.; Cochard, H.; Medlyn, B.E. On the minimum leaf conductance: Its role in models of plant water use, and ecological and environmental controls. *New Phytol.* **2019**, *221*, 693–705. [CrossRef] [PubMed]
16. Atkin, O.K.; Tjoelker, M.G. Thermal acclimation and the dynamic response of plant respiration to temperature. *Trends Plant Sci.* **2003**, *8*, 343–351. [CrossRef]
17. Fuhrer, J.; Val Martin, M.; Mills, G.; Heald, C.L.; Harmens, H.; Hayes, F.; Sharps, K.; Bender, J.; Ashmore, M.R. Current and future ozone risks to global terrestrial biodiversity and ecosystem processes. *Ecol. Evol.* **2016**, *6*, 8785–8799. [CrossRef] [PubMed]
18. Ainsworth, E.A.; Yendrek, C.R.; Sitch, S.; Collins, W.J.; Emberson, L.D. The effects of tropospheric ozone on net primary productivity and implications for climate change. *Annu. Rev. Plant Biol.* **2012**, *63*, 637–661. [CrossRef] [PubMed]
19. Li, Y.; Woo, S.Y.; Lee, J.K.; Kwak, M.J.; Khaine, I.; Jang, J.H.; Kim, H.N.; Kim, J.E.; Park, S.H.; Kim, H.D.; et al. Effects of elevated ozone on physiological, biochemical and morphological characteristics of eggplant. *Hortic. Environ. Biotechnol.* **2019**, *60*, 809–820. [CrossRef]
20. Sarkar, A.; Rakwal, R.; Agrawal, S.B.; Shibato, J.; Ogawa, Y.; Yoshida, Y.; Kumar Agrawal, G.; Agrawal, M. Investigating the impact of elevated levels of ozone on tropical wheat using integrated phenotypical, physiological, biochemical, and proteomics approaches. *J. Proteome Res.* **2010**, *9*, 4565–4584. [CrossRef]
21. Ainsworth, E.A. Understanding and improving global crop response to ozone pollution. *Plant J.* **2017**, *90*, 886–897. [CrossRef] [PubMed]

22. Paoletti, E.; Grulke, N.E. Does living in elevated CO_2 ameliorate tree response to ozone? A review on stomatal responses. *Environ. Pollut.* **2005**, *137*, 483–493. [CrossRef] [PubMed]
23. Schauberger, B.; Rolinski, S.; Schaphoff, S.; Müller, C. Global historical soybean and wheat yield loss estimates from ozone pollution considering water and temperature as modifying effects. *Agric. For. Meteorol.* **2019**, *265*, 1–15. [CrossRef]
24. Hoshika, Y.; De Carlo, A.; Baraldi, R.; Neri, L.; Carrari, E.; Agathokleous, E.; Zhang, L.; Fares, S.; Paoletti, E. Ozone-induced impairment of night-time stomatal closure in O_3-sensitive poplar clone is affected by nitrogen but not by phosphorus enrichment. *Sci. Total Environ.* **2019**, *692*, 713–722. [CrossRef] [PubMed]
25. McAinsh, M.R.; Evans, N.H.; Montgomery, L.T.; North, K.A. Calcium signalling in stomatal responses to pollutants. *New Phytol.* **2002**, *153*, 441–447. [CrossRef]
26. Hoshika, Y.; Carriero, G.; Feng, Z.; Zhang, Y.; Paoletti, E. Determinants of stomatal sluggishness in ozone-exposed deciduous tree species. *Sci. Total Environ.* **2014**, *481*, 453–458. [CrossRef] [PubMed]
27. Wilkinson, S.; Davies, W.J. Drought, ozone, ABA and ethylene: New insights from cell to plant to community. *Plant Cell Environ.* **2010**, *33*, 510–525. [CrossRef]
28. Frenck, G.; van der Linden, L.; Mikkelsen, T.N.; Brix, H.; Jørgensen, R.B. Increased [CO_2] does not compensate for negative effects on yield caused by higher temperature and [O_3] in *Brassica napus* L. *Eur. J. Agron.* **2011**, *35*, 127–134. [CrossRef]
29. Steiner, A.L.; Davis, A.J.; Sillman, S.; Owen, R.C.; Michalak, A.M.; Fiore, A.M. Observed suppression of ozone formation at extremely high temperatures due to chemical and biophysical feedbacks. *Proc. Natl. Acad. Sci. USA* **2010**, *107*, 19685–19690. [CrossRef] [PubMed]
30. Vukovich, F.M.; Sherwell, J. An examination of the relationship between certain meteorological parameters and surface ozone variations in the Baltimore-Washington corridor. *Atmos. Environ.* **2003**, *37*, 971–981. [CrossRef]
31. Qaderi, M.M.; Reid, D.M. Growth and physiological responses of canola (*Brassica napus*) to UV-B and CO_2 under controlled environment conditions. *Physiol. Plant.* **2005**, *125*, 247–259. [CrossRef]
32. Yadav, D.S.; Mishra, A.K.; Rai, R.; Chaudhary, N.; Mukherjee, A.; Agrawal, S.B.; Agrawal, M. Responses of an old and a modern Indian wheat cultivar to future O_3 level: Physiological, yield and grain quality parameters. *Environ. Pollut.* **2020**, *259*, 113939. [CrossRef]
33. Farrell, K.T. *Spices, Condiments, and Seasonings*, 2nd ed.; Springer Science & Business Media: Berlin/Heidelberg, Germany, 1999; pp. 138–140.
34. Black, V.J.; Stewart, C.A.; Roberts, J.A.; Black, C.R. Timing of exposure to ozone affects reproductive sensitivity and compensatory ability in Brassica campestris. *Environ. Exp. Bot.* **2012**, *75*, 225–234. [CrossRef]
35. Bosac, C.; Robert, J.A.; Black, V.J.; Black, C.R. Impact of O_3 and SO_2 on reproductive development in oilseed rape (*Brassica napus* L.). *New Phytol.* **1994**, *126*, 71–79. [CrossRef]
36. Singh, S.; Agrawal, S.B. Use of ethylene diurea (EDU) in assessing the impact of ozone on growth and productivity of five cultivars of Indian wheat (Triticum aestivum L.). *Environ. Monit. Assess.* **2009**, *159*, 125–141. [CrossRef]
37. Singh, P.; Agrawal, M.; Agrawal, S.B. Evaluation of physiological, growth and yield responses of a tropical oil crop (*Brassica campestris* L. var. Kranti) under ambient ozone pollution at varying NPK levels. *Environ. Pollut.* **2009**, *157*, 871–880. [CrossRef] [PubMed]
38. Singh, S.; Bhatia, A.; Tomer, R.; Kumar, V.; Singh, B.; Singh, S.D. Synergistic action of tropospheric ozone and carbon dioxide on yield and nutritional quality of Indian mustard (Brassica juncea (L.) Czern.). *Environ. Monit. Assess.* **2013**, *185*, 6517–6529. [CrossRef] [PubMed]
39. Lee, J.K.; Woo, S.Y.; Kwak, M.J.; Park, S.H.; Kim, H.D.; Lim, Y.J.; Park, J.H.; Lee, K.A. Effects of elevated temperature and ozone in *Brassica juncea* L.: Growth, physiology, and ROS accumulation. *Forests* **2020**, *11*, 68. [CrossRef]
40. National Institute of Environmental Research. *Annual Report of Air Quality in Korea 2016*; National Institute of Environmental Research: Incheon, Korea, 2017.
41. Hatfield, J.L.; Prueger, J.H. Temperature extremes: Effect on plant growth and development. *Weather Clim. Extrem.* **2015**, *10*, 4–10. [CrossRef]
42. Angadi, S.V.; Cutforth, H.W.; Miller, P.R.; McConkey, B.G.; Entz, M.H.; Brandt, S.A.; Volkmar, K.M. Response of three brassica species to high temperature stress during reproductive growth. *Can. J. Plant Sci.* **2000**, *80*, 693–701. [CrossRef]
43. Qaderi, M.M.; Kurepin, L.V.; Reid, D.M. Growth and physiological responses of canola (*Brassica napus*) to three components of global climate change: Temperature, carbon dioxide and drought. *Physiol. Plant.* **2006**, *128*, 710–721. [CrossRef]
44. Sharkey, T.D.; Bernacchi, C.J.; Farquhar, G.D.; Singaas, E.L. Fitting photosynthetic carbon dioxide response curves for C_3 leaves. *Plant. Cell Environ.* **2007**, *30*, 1035–1040. [CrossRef] [PubMed]
45. Strasser, R.J.; Tsimilli-Michael, M.; Srivastava, A. *Analysis of the Chlorophyll a Fluorescence Transient*; Springer: Dordrecht, The Netherlands, 2004; pp. 321–362.
46. Jiang, H.X.; Chen, L.S.; Zheng, J.G.; Han, S.; Tang, N.; Smith, B.R. Aluminum-induced effects on Photosystem II photochemistry in Citrus leaves assessed by the chlorophyll *a* fluorescence transient. *Tree Physiol.* **2008**, *28*, 1863–1871. [CrossRef]
47. Arnon, D.I. Copper enzymes in isolated chloroplasts. Polyphenoloxidase in *Beta vulgaris*. *Plant Physiol.* **1949**, *24*, 1–15. [CrossRef] [PubMed]
48. Venketeswaran, S. Studies on the isolation of green pigmented callus tissue of tobacco and its continued maintenance in suspension cultures. *Physiol. Plant.* **1965**, *18*, 776–789. [CrossRef]

49. Hu, X.; Tanaka, A.; Tanaka, R. Simple extraction methods that prevent the artifactual conversion of chlorophyll to chlorophyllide during pigment isolation from leaf samples. *Plant Methods* **2013**, *9*, 1–13. [CrossRef] [PubMed]
50. Xia, X.J.; Wang, Y.J.; Zhou, Y.H.; Tao, Y.; Mao, W.H.; Shi, K.; Asami, T.; Chen, Z.; Yu, J.Q. Reactive oxygen species are involved in brassinosteroid-induced stress tolerance in cucumber. *Plant Physiol.* **2009**, *150*, 801–814. [CrossRef]
51. Calatayud, V.; García-Breijo, F.J.; Cervero, J.; Reig-Armiñana, J.; Sanz, M.J. Physiological, anatomical and biomass partitioning responses to ozone in the Mediterranean endemic plant *Lamottea dianae*. *Ecotoxicol. Environ. Saf.* **2011**, *74*, 1131–1138. [CrossRef] [PubMed]
52. Gao, F.; Calatayud, V.; García-Breijo, F.; Reig-Armiñana, J.; Feng, Z. Effects of elevated ozone on physiological, anatomical and ultrastructural characteristics of four common urban tree species in China. *Ecol. Indic.* **2016**, *67*, 367–379. [CrossRef]
53. Cho, S.; Ser-Oddamba, B.; Batkhuu, N.-O.; Seok Kim, H. Comparison of water use efficiency and biomass production in 10-year-old *Populus sibirica* and *Ulmus pumila* plantations in Lun soum, Mongolia. *For. Sci. Technol.* **2019**, *15*, 147–158. [CrossRef]
54. Pell, E.J.; Eckardt, N.A.; Glick, R.E. Biochemical and molecular basis for impairment of photosynthetic potential. *Photosynth. Res.* **1994**, *39*, 453–462. [CrossRef] [PubMed]
55. Calatayud, V.; Marco, F.; Cerveró, J.; Sánchez-Peña, G.; Sanz, M.J. Contrasting ozone sensitivity in related evergreen and deciduous shrubs. *Environ. Pollut.* **2010**, *158*, 3580–3587. [CrossRef] [PubMed]
56. Glick, R.E.; Schlagnhaufer, C.D.; Arteca, R.N.; Pell, E.J. Ozone-induced ethylene emission accelerates the loss of ribulose-1,5-bisphosphate carboxylase/oxygenase and nuclear-encoded mRNAs in senescing potato leaves. *Plant Physiol.* **1995**, *109*, 891–898. [CrossRef] [PubMed]
57. Thwe, A.A.; Vercambre, G.; Gautier, H.; Gay, F.; Phattaralerphong, J.; Kasemsap, P. Response of photosynthesis and chlorophyll fluorescence to acute ozone stress in tomato (*Solanum lycopersicum* Mill.). *Photosynthetica* **2014**, *52*, 105–116. [CrossRef]
58. Makino, A.; Osmond, B. Effects of nitrogen nutrition on nitrogen partitioning between chloroplasts and mitochondria in pea and wheat. *Plant Physiol.* **1991**, *96*, 355–362. [CrossRef] [PubMed]
59. Shang, B.; Xu, Y.; Dai, L.; Yuan, X.; Feng, Z. Elevated ozone reduced leaf nitrogen allocation to photosynthesis in poplar. *Sci. Total Environ.* **2019**, *657*, 169–178. [CrossRef] [PubMed]
60. Feller, U.; Crafts-Brandner, S.J.; Salvucci, M.E. Moderately high temperatures inhibit ribulose-1,5-bisphosphate carboxylase/oxygenase (Rubisco) activase-mediated activation of Rubisco. *Plant Physiol.* **1998**, *116*, 539–546. [CrossRef] [PubMed]
61. Ferguson, J.N.; McAusland, L.; Smith, K.E.; Price, A.H.; Wilson, Z.A.; Murchie, E.H. Rapid temperature responses of photosystem II efficiency forecast genotypic variation in rice vegetative heat tolerance. *Plant J.* **2020**. [CrossRef] [PubMed]
62. Sharwood, R.E.; Crous, K.Y.; Whitney, S.M.; Ellsworth, D.S.; Ghannoum, O. Linking photosynthesis and leaf N allocation under future elevated CO_2 and climate warming in *Eucalyptus globulus*. *J. Exp. Bot.* **2017**, *68*, erw484. [CrossRef]
63. Yamori, W.; Hikosaka, K.; Way, D.A. Temperature response of photosynthesis in C_3, C_4, and CAM plants: Temperature acclimation and temperature adaptation. *Photosynth. Res.* **2014**, *119*, 101–117. [CrossRef]
64. Huntingford, C.; Atkin, O.K.; Martinez-De La Torre, A.; Mercado, L.M.; Heskel, M.A.; Harper, A.B.; Bloomfield, K.J.; O'Sullivan, O.S.; Reich, P.B.; Wythers, K.R.; et al. Implications of improved representations of plant respiration in a changing climate. *Nat. Commun.* **2017**, *8*, 1–11. [CrossRef]
65. Booker, F.L.; Burkey, K.O.; Pursley, W.A.; Heagle, A.S. Elevated carbon dioxide and ozone effects on peanut: I. Gas-exchange, biomass, and leaf chemistry. *Crop Sci.* **2007**, *47*, 1475–1487. [CrossRef]
66. Sun, J.; Feng, Z.; Ort, D.R. Impacts of rising tropospheric ozone on photosynthesis and metabolite levels on field grown soybean. *Plant Sci.* **2014**, *226*, 147–161. [CrossRef]
67. Eichelmann, H.; Oja, V.; Rasulov, B.; Padu, E.; Bichele, I.; Pettai, H.; Möls, T.; Kasparova, I.; Vapaavuori, E.; Laisk, A. Photosynthetic parameters of birch (*Betula pendula* Roth) leaves growing in normal and in CO_2- and O_3-enriched atmospheres. *Plant Cell Environ.* **2004**, *27*, 479–495. [CrossRef]
68. Xu, Y.; Feng, Z.; Tarvainen, L.; Shang, B.; Dai, L.; Uddling, J. Mesophyll conductance limitation of photosynthesis in poplar under elevated ozone. *Sci. Total Environ.* **2019**, *657*, 136–145. [CrossRef] [PubMed]
69. Flexas, J.; Ribas-Carbó, M.; Diaz-Espejo, A.; Galmés, J.; Medrano, H. Mesophyll conductance to CO_2: Current knowledge and future prospects. *Plant Cell Environ.* **2008**, *31*, 602–621. [CrossRef]
70. Paoletti, E.; Contran, N.; Bernasconi, P.; Günthardt-Goerg, M.S.; Vollenweider, P. Structural and physiological responses to ozone in Manna ash (*Fraxinus ornus* L.) leaves of seedlings and mature trees under controlled and ambient conditions. *Sci. Total Environ.* **2009**, *407*, 1631–1643. [CrossRef]
71. Xiong, D.; Douthe, C.; Flexas, J. Differential coordination of stomatal conductance, mesophyll conductance, and leaf hydraulic conductance in response to changing light across species. *Plant. Cell Environ.* **2018**, *41*, 436–450. [CrossRef] [PubMed]
72. Rai, R.; Agrawal, M.; Agrawal, S.B. Effects of ambient O_3 on wheat during reproductive development: Gas exchange, photosynthetic pigments, chlorophyll fluorescence, and carbohydrates. *Photosynthetica* **2011**, *49*, 285–294. [CrossRef]
73. Welfare, K.; Flowers, T.J.; Taylor, G.; Yeo, A.R. Additive and antagonistic effects of ozone and salinity on the growth, ion contents and gas exchange of five varieties of rice (*Oryza sativa* L.). *Environ. Pollut.* **1996**, *92*, 257–266. [CrossRef]
74. Agrawal, M.; Krizek, D.T.; Agrawal, S.B.; Kramer, G.F.; Lee, E.H.; Mirecki, R.M.; Rowland, R.A. Influence of Inverse Day/Night Temperature on Ozone Sensitivity and Selected Morphological and Physiological Responses of Cucumber. *J. Am. Soc. Hortic. Sci.* **1993**, *118*, 649–654. [CrossRef]

75. Donnelly, A.; Jones, M.B.; Burke, J.I.; Schnieders, B. Elevated CO_2 provides protection from O_3 induced photosynthetic damage and chlorophyll loss in flag leaves of spring wheat (*Triticum aestivum* L., cv. 'Minaret'). *Agric. Ecosyst. Environ.* **2000**, *80*, 159–168. [CrossRef]
76. Hassan, I.A. Physiological and biochemical response of potato (*Solanum tuberosum* L. cv. Kara) to O_3 and antioxidant chemicals: Possible roles of antioxidant enzymes. *Ann. Appl. Biol.* **2006**, *148*, 197–206. [CrossRef]
77. Pandey, A.K.; Ghosh, A.; Agrawal, M.; Agrawal, S.B. Effect of elevated ozone and varying levels of soil nitrogen in two wheat (*Triticum aestivum* L.) cultivars: Growth, gas-exchange, antioxidant status, grain yield and quality. *Ecotoxicol. Environ. Saf.* **2018**, *158*, 59–68. [CrossRef]
78. Singh, E.; Rai, R.; Pandey, B.; Agrawal, M. Development of resistance in two wheat cultivars against constant fumigation of ozone. *Proc. Natl. Acad. Sci. India Sect. B Biol. Sci.* **2018**, *88*, 1121–1134. [CrossRef]
79. Atherton, J.; Olascoaga, B.; Alonso, L.; Porcar-Castell, A. Spatial variation of leaf optical properties in a boreal forest is influenced by species and light environment. *Front. Plant Sci.* **2017**, *8*, 309. [CrossRef] [PubMed]
80. Czuba, M.; Ormrod, D.P. Effects of cadmium and zinc on ozone-induced phytotoxicity in cress and lettuce. *Can. J. Bot.* **1974**, *52*, 645–649. [CrossRef]
81. Pellegrini, E.; Nali, C.; Lorenzini, G. Ecophysiology of *Tilia Americana* under ozone fumigation. *Atmos. Pollut. Res.* **2013**, *4*, 142–146. [CrossRef]
82. Murata, N.; Takahashi, S.; Nishiyama, Y.; Allakhverdiev, S.I. Photoinhibition of photosystem II under environmental stress. *Biochim. Biophys. Acta Bioenerg.* **2007**, *1767*, 414–421. [CrossRef] [PubMed]
83. Marzuoli, R.; Finco, A.; Chiesa, M.; Gerosa, G. A dose-response relationship for marketable yield reduction of two lettuce (*Lactuca sativa* L.) cultivars exposed to tropospheric ozone in Southern Europe. *Environ. Sci. Pollut. Res.* **2017**, *24*, 26249–26258. [CrossRef] [PubMed]
84. Maliba, B.G.; Inbaraj, P.M.; Berner, J.M. The use of OJIP fluorescence transients to monitor the effect of elevated ozone on biomass of Canola Plants. *Water. Air. Soil Pollut.* **2019**, *230*, 1–12. [CrossRef]
85. Calatayud, A.; Iglesias, D.J.; Talon, M.; Barreno, E. Effects of long-term ozone exposure on citrus: Chlorophyll *a* fluorescence and gas exchange. *Photosynthetica* **2006**, *44*, 548–554. [CrossRef]
86. Walter, J.; Nagy, L.; Hein, R.; Rascher, U.; Beierkuhnlein, C.; Willner, E.; Jentsch, A. Do plants remember drought? Hints towards a drought-memory in grasses. *Environ. Exp. Bot.* **2011**, *71*, 34–40. [CrossRef]
87. Kalaji, H.M.; Jajoo, A.; Oukarroum, A.; Brestic, M.; Zivcak, M.; Samborska, I.A.; Cetner, M.D.; Łukasik, I.; Goltsev, V.; Ladle, R.J. Chlorophyll a fluorescence as a tool to monitor physiological status of plants under abiotic stress conditions. *Acta Physiol. Plant.* **2016**, *38*, 102. [CrossRef]
88. Vainonen, J.P.; Kangasjärvi, J. Plant signalling in acute ozone exposure. *Plant Cell Environ.* **2015**, *38*, 240–252. [CrossRef] [PubMed]
89. Shang, B.; Xu, Y.; Peng, J.; Agathokleous, E.; Feng, Z. High nitrogen addition decreases the ozone flux by reducing the maximum stomatal conductance in poplar saplings. *Environ. Pollut.* **2021**, *272*, 115979. [CrossRef]
90. Vollenweider, P.; Ottiger, M.; Günthardt-Goerg, M.S. Validation of leaf ozone symptoms in natural vegetation using microscopical methods. *Environ. Pollut.* **2003**, *124*, 101–118. [CrossRef]
91. Hassan, I.A.; Ashmore, M.R.; Bell, J.N.B. Effects of O_3 on the stomatal behaviour of Egyptian varieties of radish (*Raphanus sativus* L. cv. Baladey) and turnip (*Brassica rapa* L. cv. Sultani). *New Phytol.* **1994**, *128*, 243–249. [CrossRef]
92. Neufeld, H.S.; Sullins, A.; Sive, B.C.; Lefohn, A.S. Spatial and temporal patterns of ozone at Great Smoky Mountains National Park and implications for plant responses. *Atmos. Environ. X* **2019**, *2*, 100023. [CrossRef]
93. Baek, S.G.; Park, J.H.; Na, C.S.; Lee, B.; Cheng, H.C.; Woo, S.Y. The morphological characteristics of *Pterocarpus indicus* induced by elevated ozone under well-watered and drought conditions. *For. Sci. Technol.* **2018**, *14*, 105–111. [CrossRef]
94. Frey, B.; Scheidegger, C.; Günthardt-Goerg, M.S.; Matyssek, R. The effects of ozone and nutrient supply on stomatal response in birch (*Betula pendula*) leaves as determined by digital image-analysis and X-ray microanalysis. *New Phytol.* **1996**, *132*, 135–143. [CrossRef]
95. Wu, G.; Liu, H.; Hua, L.; Luo, Q.; Lin, Y.; He, P.; Feng, S.; Liu, J.; Ye, Q. Differential responses of stomata and photosynthesis to elevated temperature in two co-occurring subtropical forest tree species. *Front. Plant Sci.* **2018**, *9*, 467. [CrossRef] [PubMed]
96. Apple, M.E.; Olszyk, D.M.; Ormrod, D.P.; Lewis, J.; Southworth, D.; Tingey, D.T. Morphology and stomatal function of Douglas fir needles exposed to climate change: Elevated CO_2 and temperature. *Int. J. Plant Sci.* **2000**, *161*, 127–132. [CrossRef] [PubMed]
97. Jumrani, K.; Bhatia, V.S.; Pandey, G.P. Impact of elevated temperatures on specific leaf weight, stomatal density, photosynthesis and chlorophyll fluorescence in soybean. *Photosynth. Res* **2017**, *3*, 333–350. [CrossRef] [PubMed]
98. Baek, S.G.; Park, J.H.; Kwak, M.J.; Lee, J.K.; Na, C.S.; Lee, B.; Woo, S.Y. Physiological and biochemical responses of elevated ozone on *Pterocarpus indicus* under well-watered and drought conditions. *For. Sci. Technol.* **2018**, *14*, 153–159. [CrossRef]
99. Mukherjee, A.; Agrawal, S.B.; Agrawal, M. Responses of tropical tree species to urban air pollutants: ROS/RNS formation and scavenging. *Sci. Total Environ.* **2020**, *710*, 136363. [CrossRef] [PubMed]
100. del Río, L.A. ROS and RNS in plant physiology: An overview. *J. Exp. Bot.* **2015**, *66*, 2827–2837. [CrossRef] [PubMed]
101. Hasanuzzaman, M.; Bhuyan, M.H.M.B.; Parvin, K.; Bhuiyan, T.F.; Anee, T.I.; Nahar, K.; Hossen, M.S.; Zulfiqar, F.; Alam, M.M.; Fujita, M. Regulation of ROS metabolism in plants under environmental stress: A review of recent experimental evidence. *Int. J. Mol. Sci.* **2020**, *21*, 8695. [CrossRef]

102. Huang, S.; Van Aken, O.; Schwarzländer, M.; Belt, K.; Millar, A.H. The roles of mitochondrial reactive oxygen species in cellular signaling and stress response in plants. *Plant Physiol.* **2016**, *171*, 1551–1559. [CrossRef]
103. Han, Y.J.; Gharibeshghi, A.; Mewis, I.; Förster, N.; Beck, W.; Ulrichs, C. Plant responses to ozone: Effects of different ozone exposure durations on plant growth and biochemical quality of *Brassica campestris* L. ssp. chinensis. *Sci. Hortic. (Amst.)* **2020**, *262*, 108921. [CrossRef]
104. Menéndez, A.I.; Gundel, P.E.; Lores, L.M.; Martínez-Ghersa, M.A. Assessing the impacts of intra-and interspecific competition between *Triticum aestivum* and *Trifolium repens* on the species' responses to ozone. *Botany* **2017**, *95*, 923–932. [CrossRef]
105. Feng, Z.; Hu, E.; Wang, X.; Jiang, L.; Liu, X. Ground-level O_3 pollution and its impacts on food crops in China: A review. *Environ. Pollut.* **2015**, *199*, 42–48. [CrossRef] [PubMed]